Gazi University Journal of Science
GU J Sci
25(1):59-87 (2012)

ORIGINAL ARTICLE

Removal of Direct Red 81 Dye from Aqueous Solution by Native and Citric Acid Modified Bamboo Sawdust - Kinetic Study and Equilibrium Isotherm Analyses

Tabrez A. KHAN[1], Sarita DAHIYA[1] , Imran ALI[1,♠]

[1]*Department of Chemistry, Jamia Millia Islamia, Jamia Nagar, New Delhi 110 025, India*

Received:06/06/2010 Revised: 24/11/2010 Accepted:27/02/2011

ABSTRACT

Adsorption of Direct Red 81 (DR81) dye was investigated using Bamboo Sawdust (BSD) and Treated Bamboo Sawdust (TBSD) in a batch system with respect to initial dye concentration, adsorbent dose, pH, temperature and contact time. Maximum adsorption capacity (q_m) obtained from the Langmuir isotherm plots were 6.43 mg/g (89%) (DR81-BSD) and 13.83 mg/g (92%) (DR81-TBSD) at 303 K. Freundlich and Halsey models described the data more appropriately as compared to Langmuir, Dubinin-Kaganer-Radushkevich (DKR), Harkin-Jura and Temkin models. The adsorption dynamics conformed well to pseudo-second order kinetic equation. The adsorption process was controlled by both liquid-film and intra-particle diffusions. Thermodynamic parameters (ΔG^o, ΔH^o *and* ΔS^o) suggested the adsorption process to be spontaneous, endothermic with increase in randomness at solid-solution interface.

Keywords*: Treated Bamboo Sawdust, adsorption, isotherm, kinetic, intra-particle diffusion*

1. INTRODUCTION

The color contamination of the aqueous environment is not desirable from environmental, aesthetical and economical point of view. Dyes are generally synthetic organic aromatic compounds, which is embodied with various functional groups and heavy metals. Most of the industries like textile, leather, plastics, paper, food, cosmetics, etc., use dyes and pigments to color their products. The colour dye effluents are considered to be highly toxic to the aquatic biota and affect the symbiotic process by disturbing the natural equilibrium through reducing photosynthetic activity and primary production due to the coloration of the water in streams. Also, the persisting nature of color, non-biodegradable, toxic and inhibitory nature of the spent dye bath has considerable deleterious effect on the total environmental matrix [1, 2]. The complex framework of dye with the presence of heavy metals induces chronic toxicity particularly; they are mutagenic, teratogenic and carcinogenic [3]. And causes many water born diseases, such as nausea, haemorrhage, ulceration of skin and mucous membrane, dermatitis, perforation of nasal septum and severe irritation of respiratory tract [3]. For this reason, the removal of contaminants from the colored effluents is requiring prior to discharge into receiving waters.

Various techniques like precipitation, ion exchange, chemical oxidation and adsorption have been used for the removal of toxic pollutant from wastewater [4-6]. Of these methods, adsorption has been found to be an efficient and economically cheap process for removing dyes using various adsorbents. Different types of adsorbents have been employed till date, in adsorption processes used for removal of dyes from wastewater. Granulated activated carbon is one of the favorite adsorbents used. However, activated carbon is difficult to regenerate and disposal is also difficult. Now days many research are done for developing several adsorbents, which are of low cost, easy to regenerate

♠Corresponding author, e-mail: drimran_ali@yahoo.com,

and dispose for the removal of dyes from wastewater. These include, bottom ash and de-oiled soya [7-11], fly ash [12], akash kinari coal [13], bagasse fly ash [14], carbon slurry [15], wheat husk [16], non-living algal biomass Oedogonium sp. [17], charfines [18], banana pith [19], activated rice husk [20], coir pith [21] and activated carbon and activated rice husks [22]. Such adsorbents have given satisfactory performance in laboratory scale for treatment of colored effluents.

Plant biomass is a natural renewable resource that can be converted into useful materials and energy. Solid waste from bamboo is highly abundant in north-east region of India. It is an enduring, versatile and highly renewable material, one that people and communities have known and utilized from thousands of years. Use of bamboo to a value-added product will help to solve part of the problem of wastewater treatment. The present paper evaluates the adsorption potential of BSD and TBSD for Direct Red 81 (Figure.1) dye by optimizing all adsorption parameters that effect adsorption, such as initial dye concentration, pH, contact time, adsorbent dose and temperature.

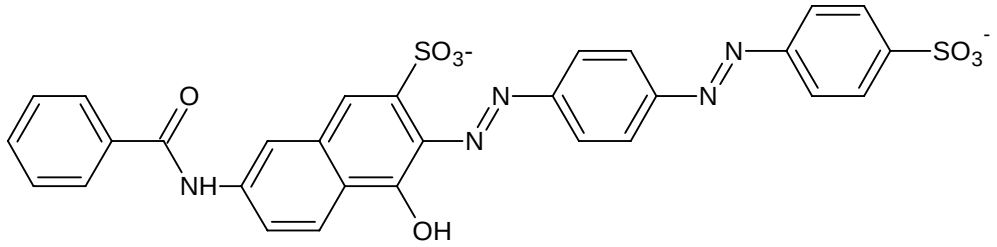

Figure 1. Chemical structure of Direct Red 81 dye.

2. MATERIALS AND METHODS

2.1. Chemicals and equipments

DR81 was obtained from (Aldrich, USA), NaOH and HCl from (Merck, Mumbai). UV-Visible spectrometer (Perkin-Elmer LamBSDa EZ-201) was used to determine the concentration of DR81 dye at 508 nm λ_{max}. The stock solution of Direct Red 81 (1000 mg/L) was prepared in double distilled water and further diluted to various low concentration solutions. pH was recorded with the pH meter (model 611, Orion Research Inc., USA). The XRD analysis was carried out using PW 1830 apparatus (PANalytical) with monochromated $CuK_{\alpha 1}$ radiation. IR spectra were recorded with FTIR spectrophotometer (Perkin Elmer 3*λ)*. Scanning electron micrograph (SEM) of the adsorbents was recorded with JEOL model 3300 microscope.

2.2 Preparation of adsorbent

Raw material (bamboo) was procured locally and washed repeatedly with water to remove dust and soluble impurities and were allowed to dry first at room temperature in shade and then in an air oven at 80-90 ^{o}C, so long as it become crispy. Then it was crushed into fine powder in a mechanical grinder and was sieved in to fractions of 75-150 µm. Then washed further with double distilled water till the washings were free of color and turbidity. After sun drying for several hours these fractions were preserved in glass bottles for use as BSD adsorbent. Then take 100 g of bamboo sawdust and soaked in 0.6M citric acid for 2 hours at 20 ^{o}C. The acid-dust slurry was dried overnight at 50 ^{o}C and then the dried husk was heated to 120 ^{o}C. The reacted product was washed repeatedly with distilled water (200 mL per g of sawdust) to remove any excess of citric acid followed by oven drying overnight at 100 ^{o}C.

2.3 Adsorption experiments

The stock solution of DR81 (1000 mg/L) was prepared in double distilled water and further diluted to various low concentration solutions ranging from 5 to 60 mg/L. Adsorption experiments were carried out at fixed agitation speed at room temperature (303 K) under batch mode as per the experimental conditions detailed in Table 2. By varying the following experimental parameters keeping the other parameters constant, five different sets of adsorption experiments were carried out (Table 2).

1. initial concentration of dye
2. contact time
3. dose of adsorbent
4. initial pH of the dye solution
5. temperature

In a batch method a fixed amount of the adsorbent dose was added to 50 mL DR81dye solution of varying concentrations, in 250 mL conical flasks. The solution was stirred in thermostatic water bath shaker at a constant speed at a given temperature. After equilibrium was attained, the adsorbate was separated from the adsorbent by centrifugation. The centrifugate was then analyzed for remaining initial adsorbate concentration at predetermined λ_{max} spectropmetrically. For kinetic measurements, the experiments were performed using a fixed adsorbent dose with varying contact times at different dye concentrations. The effect of varying solution pH (2 to 10) was also studied by adjusting pH of dye solutions with dil. HCl or NaOH solutions (both 0.01M). The experiments were repeated five time and average values were taken. Standard deviations were found to be within ± 2.2%. The amount of dye adsorbed per unit mass of the BSD/TBSD ($q_{e,}$ mg/g) was calculated using the following equation:

$q_e = (C_o - C_e) / m$ (1)

where C_o is initial dye concentration in mg/L before adsorption and m is the amount of the adsorbent (g/L of dye solution). The percentage adsorption was calculated from the relationship

$\% \text{ adsorption} = 100 (C_o - C_e) / C_o$ (2)

3. RESULTS AND DISCUSSION

3.1 .Characterization of adsorbent

The elemental composition of BSD and TBSD, as determined by Energy Dispersive X-Ray (EDX) analysis is summarized in Table 1.

Table 1.Elemental composition of bamboo sawdust and treated bamboo sawdust

	BSD		TBSD	
Element	Weight %	Atomic %	Weight %	Atomic %
C	51.20	58.78	51.23	58.80
O	46.93	40.45	46.95	40.48
Al	0.21	0.11	0.18	0.14
Si	0.94	0.46	0.91	0.42
Ca	0.36	0.12	0.35	0.10
Cu	0.37	0.08	0.38	0.06

FT-IR spectrum of the BSD (Figure. 2a) showed the most prominent peaks in the spectrum originate from hydroxyl group, which was probably attributed to adsorbed water (3854.41cm^{-1}) and CH_2 and CH_3 asymmetric and symmetric stretching vibrations (2871.80 cm^{-1}). The spectrum of the BSD also displayed number of peaks corresponding to the presence of many functional groups: NH stretch (2322.69 cm^{-1}), C=O stretching (1733.43 cm^{-1}), CO chelate stretching (1653.67 cm^{-1}), secondary amine (1507.27 cm^{-1}), symmetric bending of CH_3 (1457.25 cm^{-1}), CH_2 bending (1428.45 cm^{-1}), C-N vibration in primary amide (1368.59 cm^{-1}), C-O stretching (1272.55 cm^{-1}), O-H bending (1245.29 cm^{-1}), C-O antisymmetric stretching (1162.76 cm^{-1}), stretching of the many C-OH and C-O-C bonds (1054.53 cm^{-1}) [23], C-H (835.67 and 897.87 cm^{-1}), Al-OH deformation (787.92 cm^{-1}), Al-O deformation (671.48 cm^{-1}) and SiO (541.18 cm^{-1}). On comparing spectrum of TBSD with BSD, it could be seen that there were strong characteristic stretching vibration absorption band of carboxyl group (1732.20 cm^{-1}) and C-N vibration of primary amide (1384.3 cm^{-1}). It reflected the result of citric acid esterification (Figure. 2b). The spectrum of DR81 loaded BSD and TBSD also exhibited small shift in some bands and some bands were disappeared. The intensity of the peaks were either minimized or shifted slightly as shown in Figure. 2(a and b). These changes observed in the spectrum indicated the possible involvement of these functional groups on the surface of the BSD and TBSD in adsorption process.

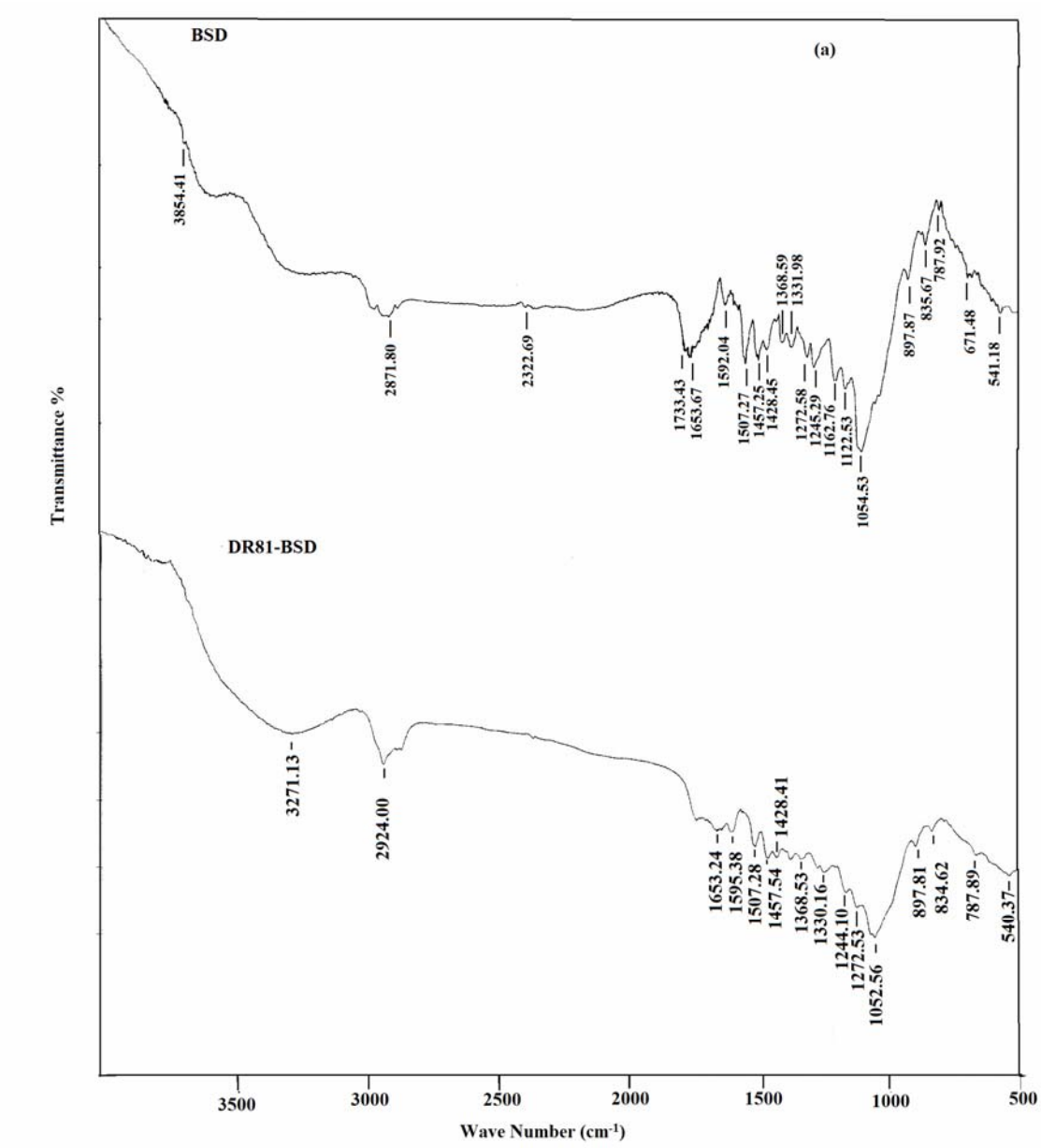
BSD
(a)
3854.41
2871.80
2322.69
1733.43
1653.67
1592.04
1507.27
1457.25
1428.45
1368.59
1331.98
1272.58
1245.29
1162.76
1122.53
1054.53
897.87
835.67
787.92
671.48
541.18
DR81-BSD
3271.13
2924.00
1653.24
1595.38
1507.28
1457.54
1428.41
1368.53
1330.16
1244.10
1272.53
1052.56
897.81
834.62
787.89
540.37
Transmittance %
3500
3000
2500
2000
1500
1000
500
Wave Number (cm-1)

(a)

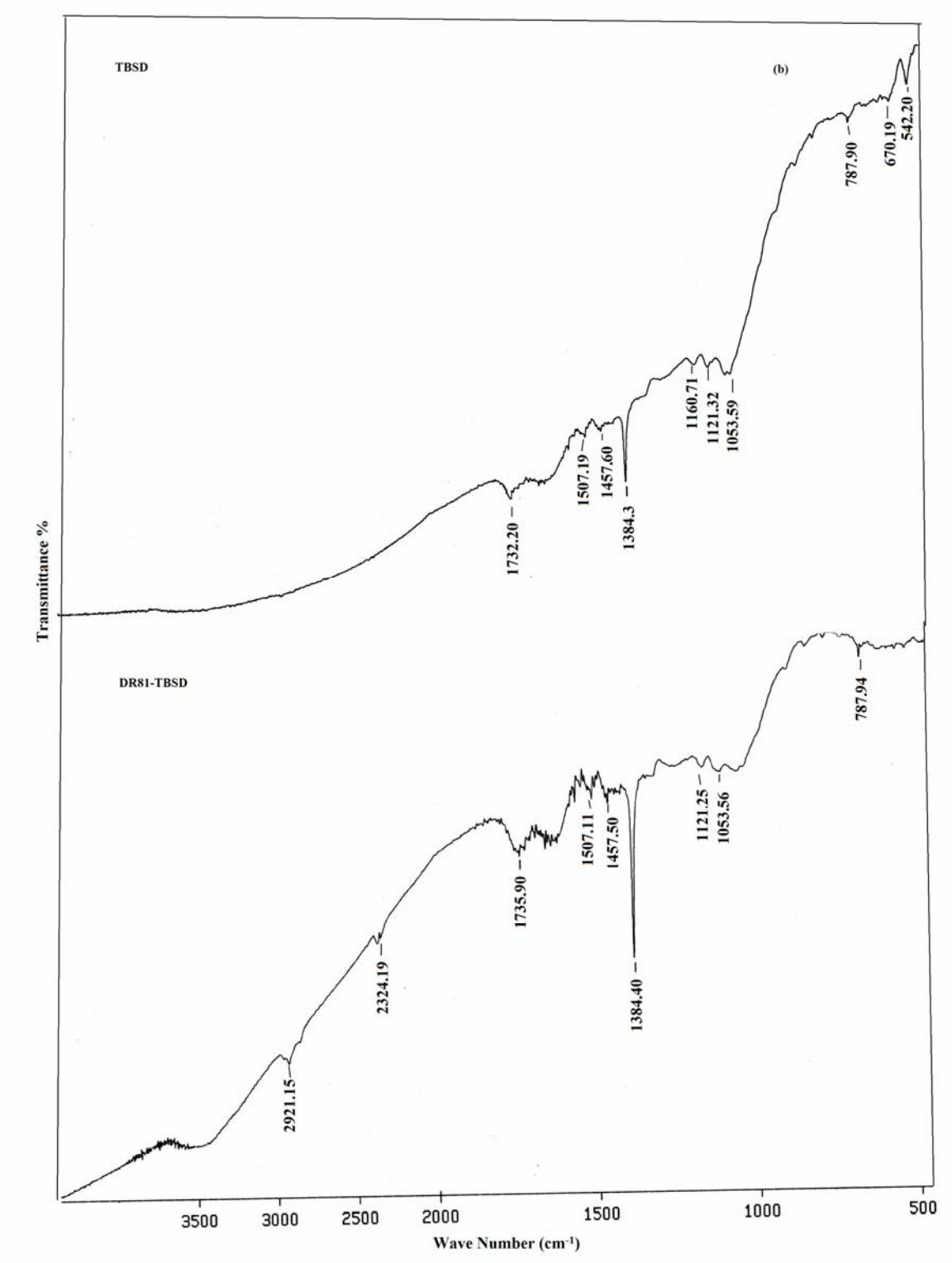

(b)

Figure 2. FTIR spectra of (a): bamboo sawdust and (b): treated bamboo sawdust before and after adsorption.

The X-ray diffraction (XRD) pattern of the BSD and TBSD, before and after adsorption, is shown in Figure. 3(a and b). The presence of intense main peak indicated the presence of some crystalline structures of the BSD and TBSD. The basal spacing of the BSD was observed at 2.3428, 2.0276, 1.4332 and 1.3882 A^0. The basal spacing observed at 2.3428 A^0, can be matched with those of Al_2O_3, whereas those found at 1.4332 and

1.3848 A^0 corresponds to SiO_2 (Figure. 3a). The basal spacing of the TBSD was observed at 4.2001, 3.0806, 2.9224, 2.5140, 2.3059, 1.9290, 1.8855, 1.8138 and 1.5270 (Figure. 3b). After adsorption, the change in diffraction pattern was clearly noticeable and new diffraction pattern was observed as shown in Figure. 3(a and b), with change in the intensity of the peaks, which might be attributed to the adsorption of dyes onto the surface of the BSD and TBSD by physiosorption.

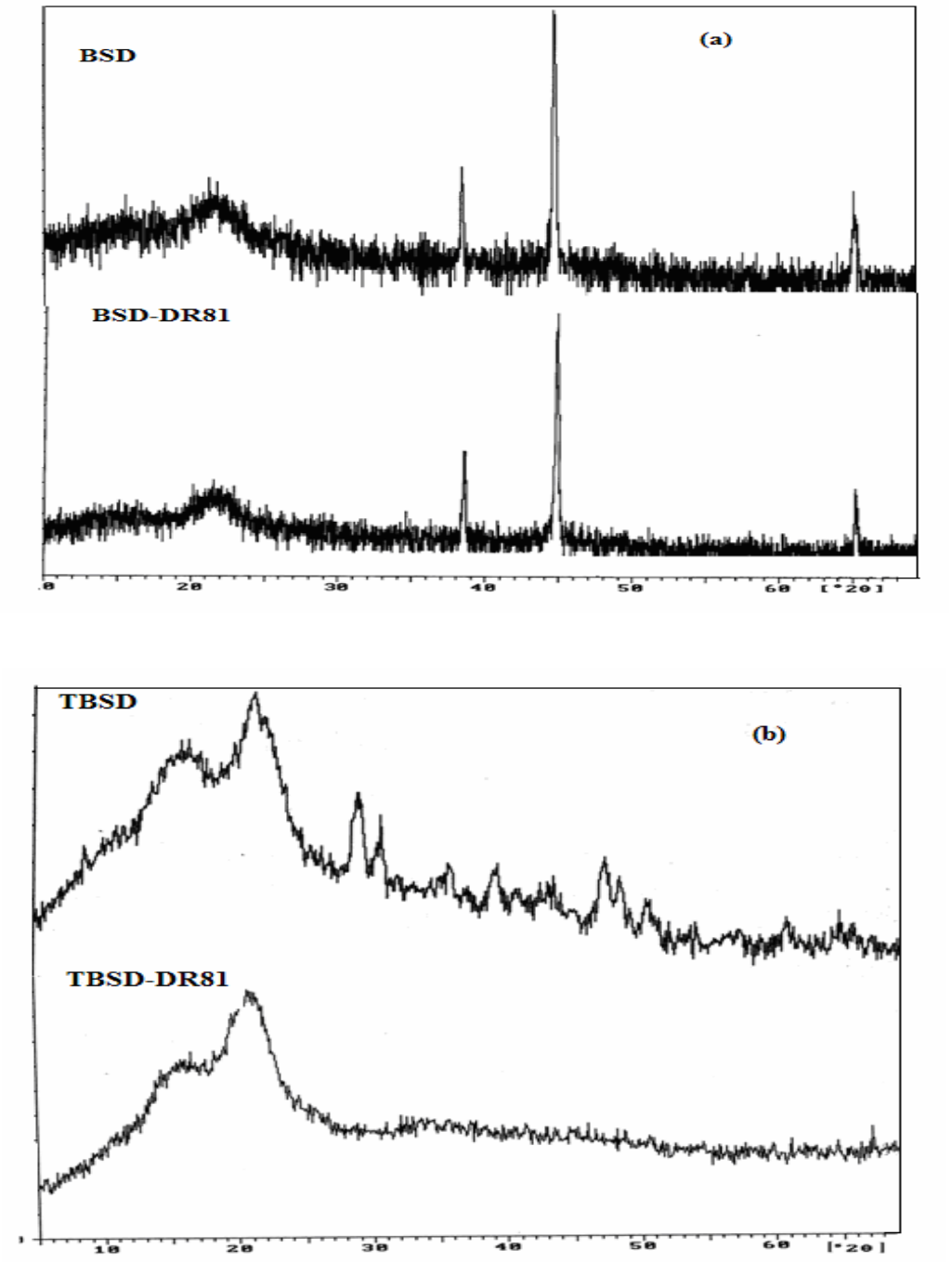

Figure 3. XRD pattern of (a): bamboo sawdust and (b): treated bamboo sawdust before and after adsorption.

Scanning Electron Microscope was used to investigate the surface morphology BSD and TBSD as shown in Figure. 4a and 4b. The SEM image before dye adsorption revealed the rough surface of BSD and TBSD. The rough surface micrograph shows ridge like structure within which the presence of the macro pores were clearly noticeable. These rough surfaces and the macro pores were responsible for the high surface area, making BSD and TBSD a good adsorbent. The SEM image of BSD and TBSD after adsorption showed smooth surface because the dye molecules were trapped and adsorbed on its surface.

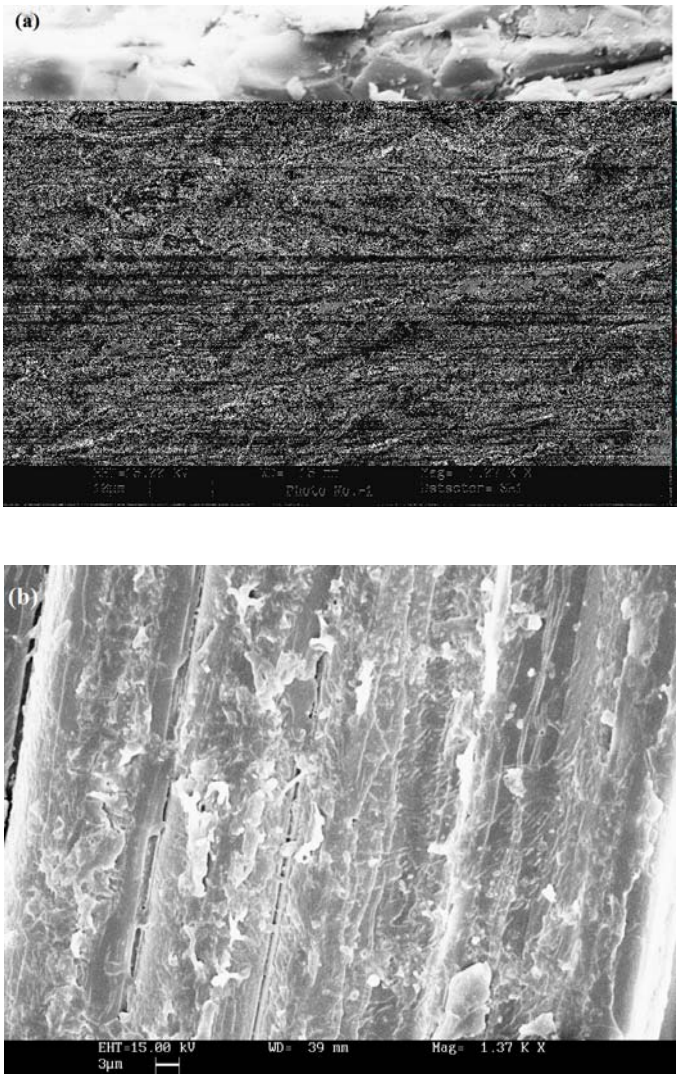

Figure 4. SEM images of (a): bamboo sawdust and (b): treated bamboo sawdust.

Table 2.Experimental conditions for the series of adsorption experiments on adsorption of Direct Red 81 onto (a): bamboo sawdust and (b): treated bamboo sawdust

Variation	Initial Concentration (mg/L)	Contact Time (min)	Dose of Adsorbent (g/L)	Initial pH	Temperature (K)
1. Initial Concentration					
(a) DR81-BSD	5-35	80	6	7	303
(b) DR81-TBSD	5-50	60	3.5	7	303
2. Contact Time (min)					
(a) DR81-BSD					
(b) DR81-TBSD	30	10-90	6	7	303
	40	10-80	3.5	7	303
3. Dose of Adsorbent (g/L)					
(a) DR81-BSD	30	80	1-8	7	303
(b) DR81-TBSD	40	60	0.5-4.5	7	303
4. Initial pH					
(a) DR81-BSD	30	80	6	2-10	303
(b) DR81-TBSD	40	60	3.5	2-10	303
5. Temperature (K)					
(a) DR81-BSD	5-30	80	6	7	303-323
(b) DR81-TBSD	5-40	60	3.5	7	303-323

3.2 Effect of pH

The studies on the removal of DR81 dye by BSD and TBSD were carried out at different pH (2-10) keeping other experimental parameters constant (Table 2). The percentage removal of dye decreased from 92.3 to 73 (DR81-BSD) and 95.3 to 77 (DR81-TBSD) with the increase in pH (Figure. 5). The solution pH, affected the surface charge of the adsorbent and thus the adsorption rate. In DR81-BSD and DR81-TBSD interaction at low pH, the adsorbent's surface was protonated by H_3O^+ ions, which provide an electrostatic attraction between the adsorbent surface (BSD or TBSD) and the DR81 dye molecules leading to maximum adsorption [24, 25]. However, when the solution pH was increased, the degree of protonation of the surface of adsorbent (BSD or TBSD) will be less which results in the decrease in diffusion and adsorption due to electrostatic repulsion [26, 27]. Similar trend was also reported for the adsorption of DR81 on cross-linked chitosan beads [28-29]. Of course, the maximum adsorption for DR81 was at low pH 2 but due to the fact that almost all water resources have pH 6-8 and this system will be useful in natural conditions, we selected pH 7 for further experiments.

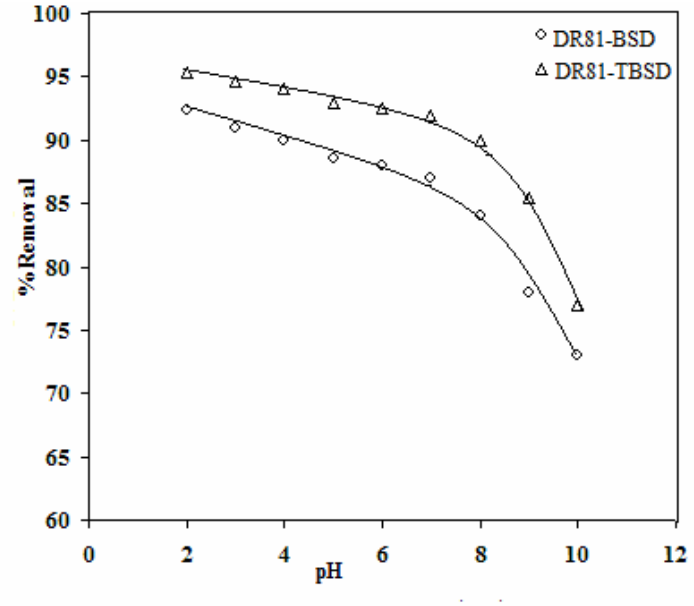

Figure 5. Effect of pH on adsorption of Direct Red 81 dye onto bamboo and treated bamboo sawdust

3.3 Equilibrium time (t)

The studies on the removal of DR81 dye by BSD and TBSD were carried out at different contact time keeping other experimental parameters constant (Table 2). The percentage removal of dye increased from 51 to 89 (DR81-BSD) and 55 to 92 (DR81-TBSD) with increase in contact time and then slowly reached the equilibrium (Figure. 6). The initial rapid adsorption might be attributed to the large number of vacant sites were available for dye molecules, and afterwards the remaining free surface sites were difficult to be occupied, because of repulsive forces between the phases. So the equilibrium time 80 min (DR81-BSD) and 60 min (DR81-TBSD) were selected as the contact time for further studies in both the adsorption system.

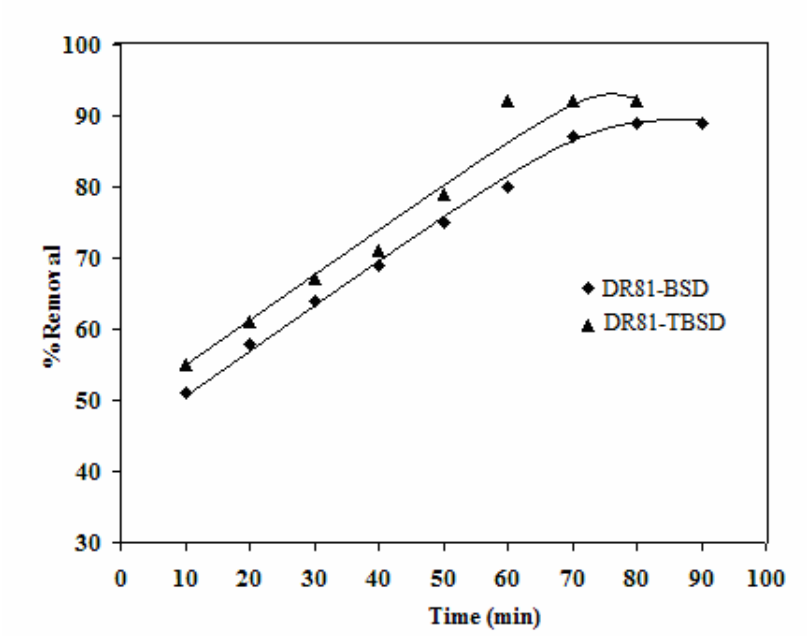

Figure 6. Effect of contact time on adsorption of Direct Red 81 dye onto bamboo and treated bamboo sawdust.

3.4 Effect of initial dye concentration

The studies on the removal of dye by BSD and TBSD were carried out at different initial concentration from 5 to 35 mg/L (DR81-BSD) and 5 to 50 mg/L (DR81-TBSD) keeping other experimental parameters constant (Table 2). The percentage removal of dye by adsorbent decreased from 97 to 89 (DR81-BSD) and 98 to 92 (DR81-TBSD) with the increased initial dye concentration (Figure. 7). This showed that the adsorption was dependent on initial concentrations of dye. It might be because at lower concentration, the ratio of the initial number of dye molecules to the available surface area was low; subsequently the

fractional adsorption became independent of initial concentration. However, at high concentration large number of dye molecules came in contact with the available adsorption sites, hence, higher number of dye molecules gets adsorbed. Thus, q_e increased while percent adsorption decreased. Thus, the maximum amount adsorbed was 3.79 mg/g (DR81-BSD) and 10.51 (DR81-TBSD) at 30 mg/L and 40 mg/L of dye concentration which was chosen for further studies.

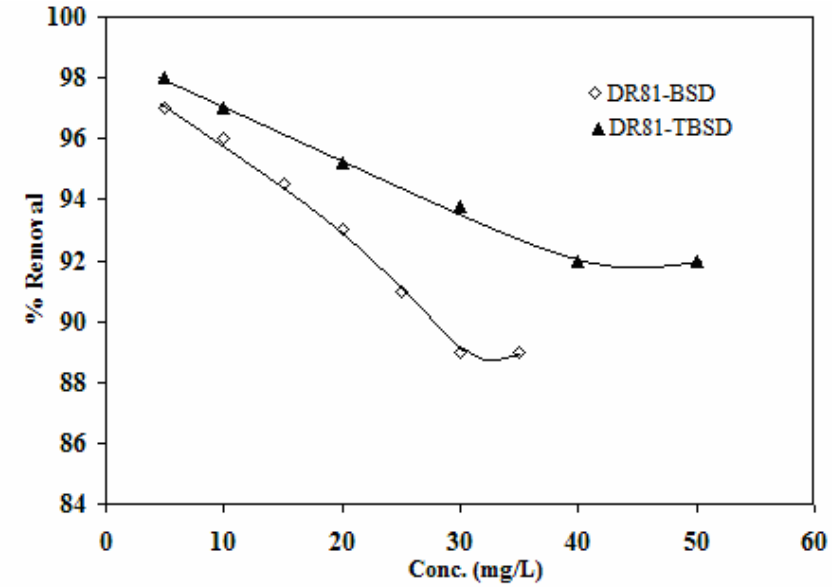

Figure. 7. Effect of initial concentration on adsorption of Direct Red 81 dye onto bamboo and treated bamboo sawdust.

3.5 Effect of dose

The studies on the removal of DR81 dye were carried out at different BSD and TBSD doses keeping other experimental parameters constant (Table 2). The percentage removal of dye increased from 70 to 89 (DR81-BSD) and 74 to 92 (DR81-TBSD) with the increase in adsorbent dose (Figure. 8). This might be attributed to the greater availability of the exchangeable sites or surface area at higher concentration of the adsorbent. So dose 6 g/L (DR81-BSD) and 3.5 g/L (DR81-TBSD) have been selected as optimized dose for further studies in both the adsorption system.

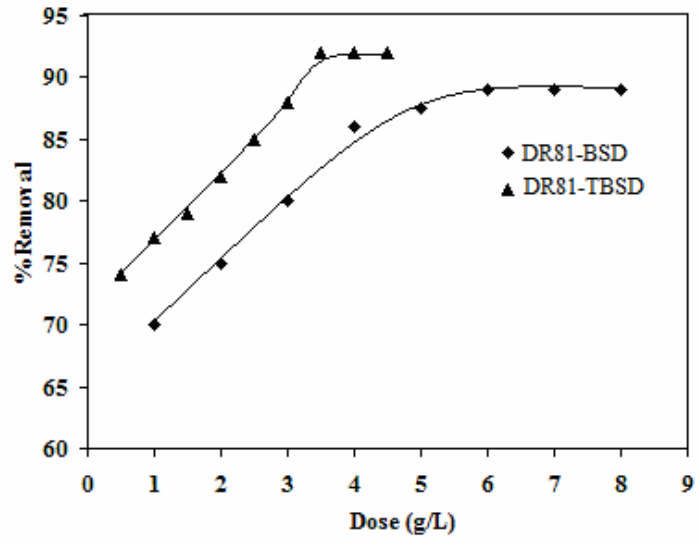

Figure. 8. Effect of adsorbent dose on adsorption Direct Red 81 dye onto bamboo and treated bamboo sawdust.

3.7. Effect of temperature

The studies on the removal of DR81 dye by BSD and TBSD were carried out at three different temperatures i.e. 303 K, 313 K and 323 K keeping other experimental parameters constant (Table 2). The percentage removal of dye increased with the increase in temperature (Figure. 9). The adsorption varies in the order: 303 K < 313 K < 323 K indicating endothermic nature of adsorption system [30]. This might be ascribed to (a) increase in the rate of diffusion of adsorbate molecules across the external boundary layer and internal pores of the adsorbent, (b) an increase in the porosity and in the total pore volume of the adsorbent with temperature, and (c) increase in the available active sites for adsorption [31]. Of course, adsorption was high at 323 K but all experiments were carried out at 303 K as most of water resources have this temperature.

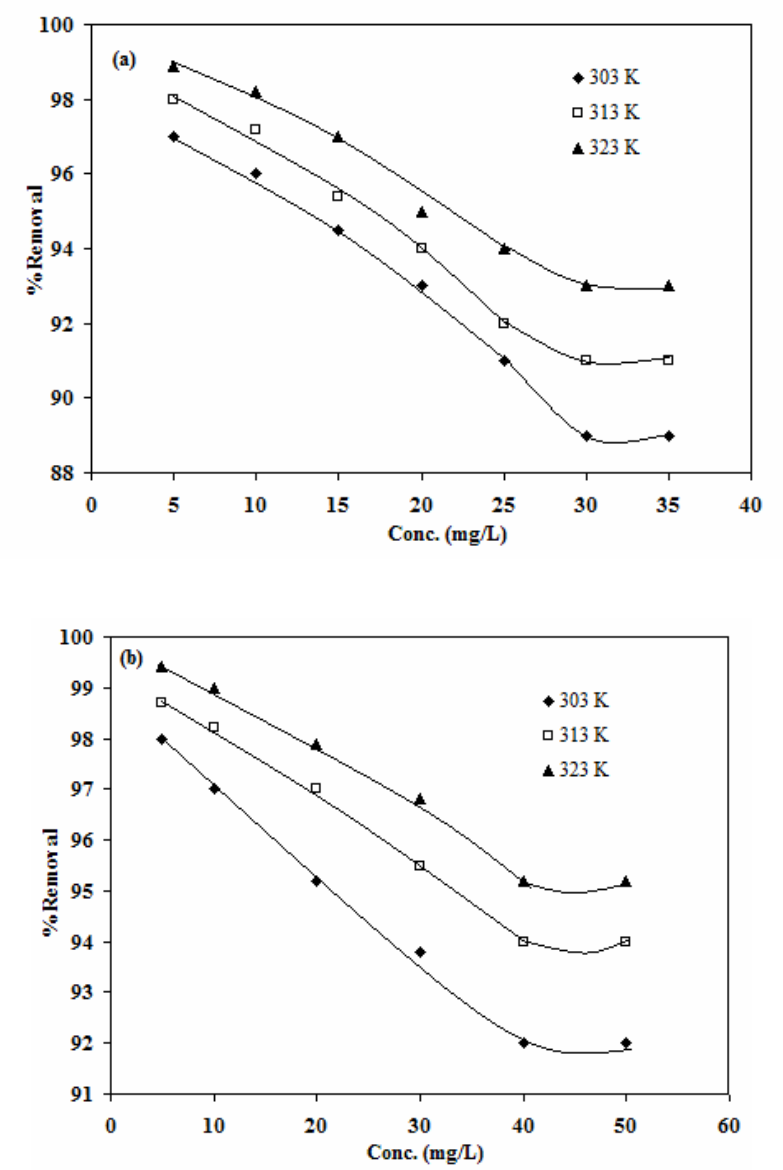

Figure 9. Effect of temperature on adsorption of Direct Red 81 onto (a): bamboo sawdust and (b): treated bamboo sawdust.

3.8 Adsorption isotherm

The results obtained from the adsorption of dye onto BSD and TBSD were analyzed by well known models of Langmuir, Freundlich, Dubinin-Kaganer-Radushkevich, Temkin, Harkin-Jura and Halsey isotherm.

3.8.1 Langmuir isotherm

Langmuir isotherm is valid for monolayer adsorption and the equation used is given below [32]:

$$C_e/q_e = 1 / (bq_m) + (1 / q_m) C_e \quad (3)$$

where C_e is equilibrium concentration of dye in solution, q_e is the amount of dye adsorbed at equilibrium, q_m is Langmuir monolayer adsorption

capacity (mg/g), and b is Langmuir constant related to equilibrium constant of the adsorption (dye + BSD/TBSD = dye--- BSD/TBSD) (L/mg). A straight line plot of C_e/q_e *vs.* C_e (Figure. 10) indicated that uptake of DR81 dye occurred on adsorbent (BSD/TBSD) homogeneous surface by monolayer adsorption without any interaction between adsorbate molecules. The slope and the intercept of the plot gave the values of q_m and b, respectively, which have been given in Table 3. The values of the dimensionless separation factor (R_L) [33], were calculated from Langmuir isotherm constants using the expression,

$$R_L = 1 / (1 + b C_0) \quad (4)$$

where C_0 is initial DR81 dye concentration in mg/L before adsorption. It is suggested that for favorable adsorption, $0 < R_L < 1$. The values of the dimensionless separation factor, (R_L) [33] varied from 5.28 to 6.43 (DR81-BSD) and 0.35 to 0.47 (DR81-TBSD) supporting favorable adsorption (Table 3). The adsorption capacity (q_m) 6.43 mg/g (89%) (DR81-BSD) and 13.83 mg/g (92%) (DR81-TBSD) were found to be higher than other adsorbents reported earlier (Table 4). So the prepared adsorbent in the present study showed efficient adsorption capacity for the removal of dyes from aqueous solution.

Table 3.Adsorption isotherm parameters for adsorption of Direct Red 81 onto (a): bamboo sawdust and (b): treated bamboo sawdust.

Isotherms	Isotherm constants	DR81-BSD			DR81-TBSD		
		303 K	313 K	323 K	303 K	313 K	323 K
Langmuir	q_m	6.43	5.49	5.28	13.83	13.38	12.53
	b	0.69	1.34	2.21	0.84	1.41	2.66
	R_L	0.30	0.21	0.17	0.47	0.43	0.35
	R^2	0.98	0.97	0.96	0.96	0.97	0.97
Freundlich	n_f	0.54	0.50	0.50	0.58	0.56	0.55
	K_f	2.47	2.80	6.79	5.49	6.71	7.20
	R^2	0.98	0.99	1	0.99	0.99	0.99
DKR	q_D	3.61	3.65	3.74	7.83	8.49	8.59
	E	2.85	3.37	4.13	3.11	3.58	4.52
	R^2	0.92	0.92	0.92	0.89	0.93	0.93
Temkin	K_t	10.95	17.02	32.00	12.53	20.26	44.70
	β	1.17	1.09	1.00	2.58	2.54	2.24
	R^2	0.98	0.96	0.95	0.94	0.96	0.95
Harkin-Jura	A	0.99	1.09	1.23	3.45	3.71	4.14
	B	0.33	0.24	0.12	0.28	0.14	0.01
	R^2	0.76	0.77	0.78	0.85	0.82	0.80
Halsey	n_h	1.82	1.98	2.18	1.71	1.78	1.85
	K_h	8.92	7.74	7.23	18.43	31.80	2.93
	R^2	0.98	0.99	0.99	0.99	0.99	0.98

Table 4.Comparison of monolayer capacities (q_m) of different adsorbents

Adsorbents	q_m (mg/g)	References	Dye
Activated hazelnut shell carbon	11	[34]	Direct yellow 50
Activated carbon	7.69	[35]	Direct brown 1
Coir pith	6.72	[21]	Direct red 28
Chemviron GW activated carbon	8.40	[36]	Direct red 89
Treated bamboo sawdust	13.83	This work	Direct Red 81
Charfines	6.4	[18]	Direct brown 1
Banana pith	5.92	[19]	Direct red
Activated rice Husk	4.35	[20]	Direct red 23
Red mud	4.05	[37]	Direct red 28
Bamboo sawdust	6.43	This work	Direct Red 81

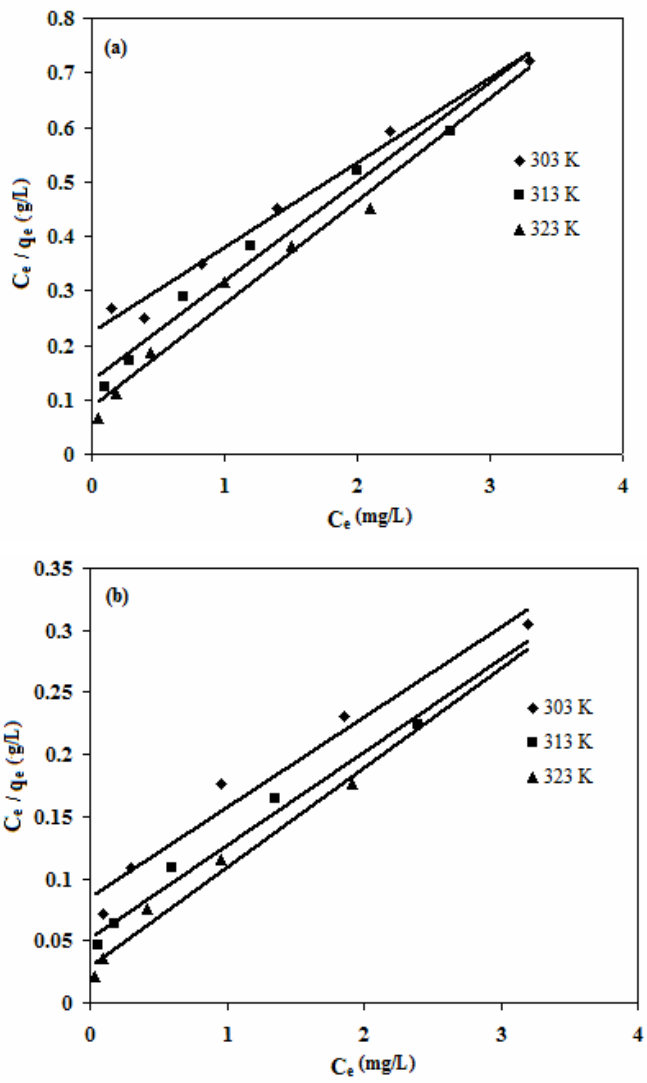

Figure 10. Langmuir adsorption isotherm plots for adsorption of Direct Red 81 onto (a): bamboo sawdust and (b): treated bamboo sawdust.

3.8.2 Freundlich isotherm

The isotherm given by the Freundlich equation is often used to describe non-specific adsorption that involves heterogeneous surfaces. This equation has the form [38]:

$$log\ q_e = log\ K_f + n_h\ log\ C_e \quad (5)$$

Where Freundlich coefficients, K_f (related to adsorption capacity) (L/g) and n_h (related to adsorption intensity) were obtained from the slope and the intercept of the linearlized Freundlich plots. Linear plots of $log\ q_e$ *vs.* $log\ C_e$ (Figure. 11) indicated that the adsorption followed Freundlich equation in both the adsorption system. The Freundlich constants K_f and n_h along with R^2 are shown in Table 3. The values of K_f lie between 2.47-6.79 L/g (DR81-BSD) and 5.49-7.20 L/g (DR81-TBSD) in the two adsorption system. And the values of $n_h < 1$ lying between 0.50-0.54 (DR81-BSD) and 0.55-0.58 (DR81-TBSD) indicated more favorable physical adsorption.

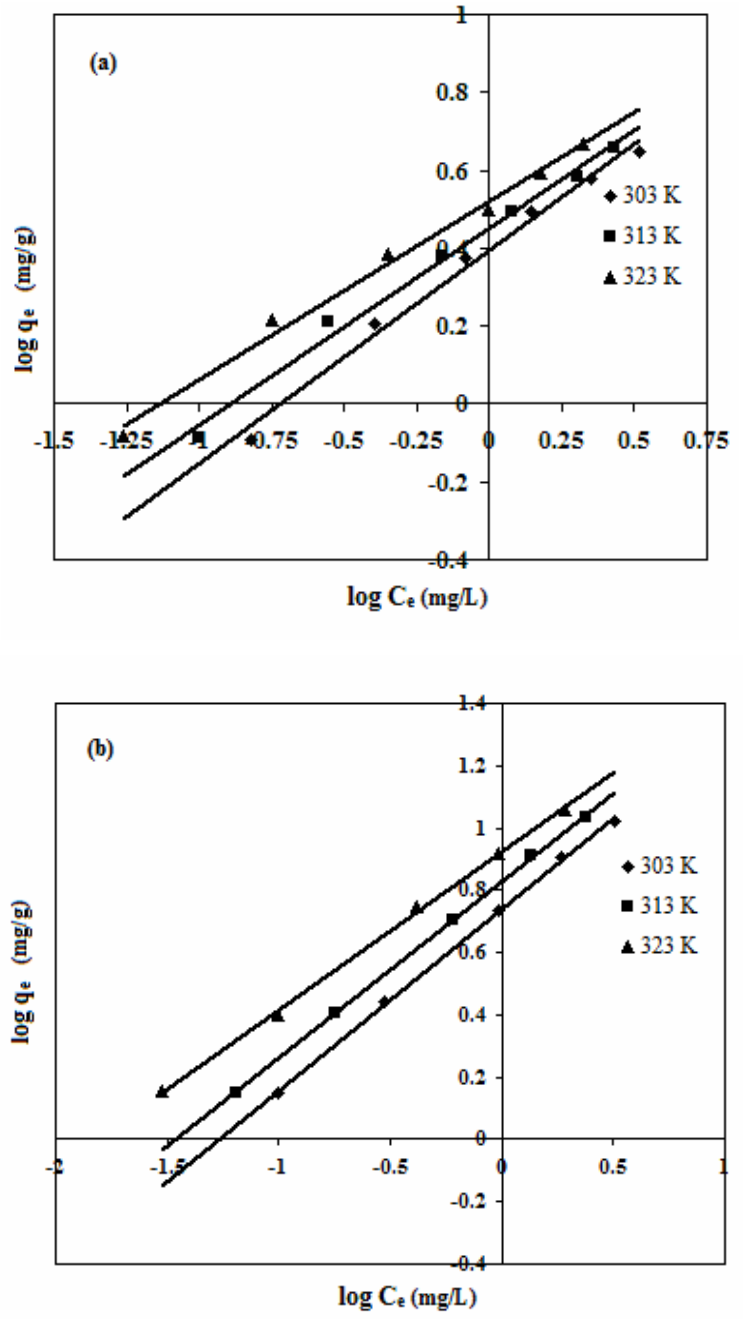

Figure. 11. Freundlich adsorption isotherm plots for adsorption of Direct Red 81 onto (a): bamboo sawdust and (b): treated bamboo sawdust.

3.8.3 Dubinin-Kaganer-Radushkevich (DKR) isotherm

The DKR model is used to estimate the characteristic porosity of the adsorbent and the apparent energy of adsorption. The model is represented by the equation [39]:

$$ln\ q_e = ln\ q_D - \beta\epsilon^2 \quad (6)$$

where q_e = amount of DR81 adsorbed per gram of BSD/TBSD, q_D = DKR isotherm constant related to degree of DR81 adsorption (mg/g), β = activity coefficient, C_e = equilibrium concentration of DR81 in mg/L and $\epsilon = RT\ ln(1+1/C_e)$ which is called as Polanyi Potential. A plot of ln q_e *vs.* ϵ^2 yielding straight line confirms the model (Figure. 12). The DKR constant can be determined from the intercept of the straight line graph. The apparent energy of adsorption is related to the activity coefficient β as follows

$$E = 1 / (2\beta)^{1/2} \quad (7)$$

Where 2β is equal to the slope of the straight line graph. The values of q_D and E, along with R^2 are given in Table 3. The mean value of adsorption capacity q_D were found to be 3.67 mg/g (DR81-BSD) and 8.30 mg/g (DR81-TBSD) which was less than the mean Langmuir adsorption capacity 5.74 mg/g (DR81-BSD)

and 13.24 mg/g (DR81-TBSD) in both the adsorption system This might be attributed to different assumptions taken into consideration while formulating the isotherms. The mean value of adsorption energy, E is useful in estimating the type of adsorption i.e. an energy range from 1.00 to 8.00 and 8.00 to 16.00 kJ/mol indicated physical and chemical adsorption, respectively. The E values lies in between 2.85-4.13 kJ/mol (DR81-BSD) and 3.11-4.52 kJ/mol (DR81-TBSD) indicated physical adsorption in both the adsorption system.

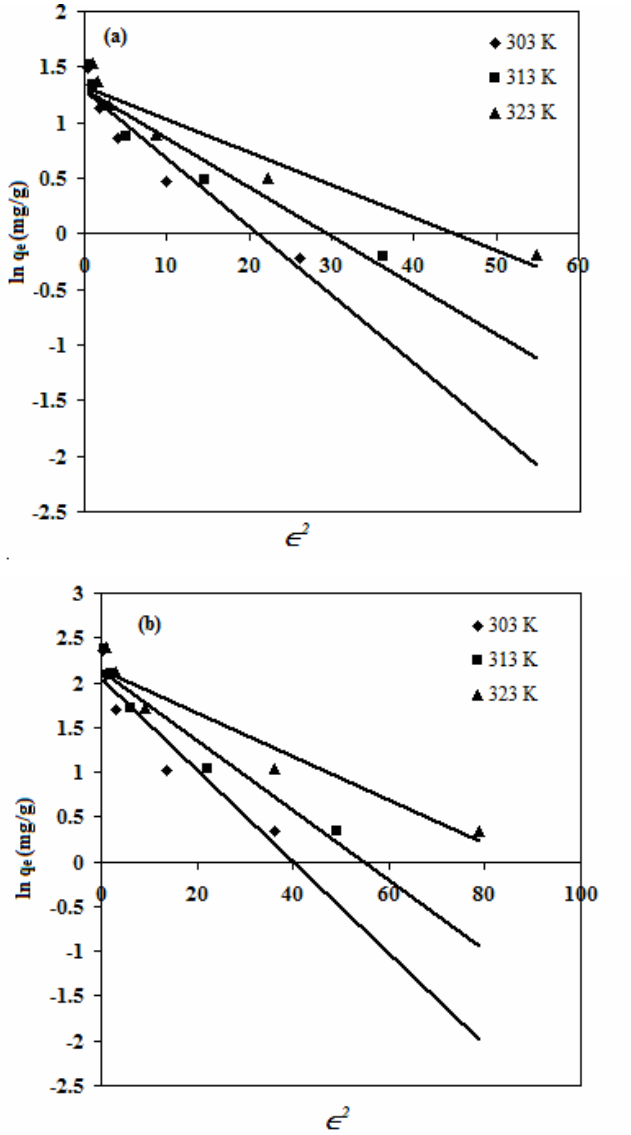

Figure 12. DKR adsorption isotherm plots for adsorption of Direct Red 81 onto (a): bamboo sawdust and (b): treated bamboo sawdust.

3.8.4 Temkin isotherm

Temkin isotherm (Eq. 8) assumes that the heat of adsorption of all the molecules in the layer decreases linearly with coverage due to adsorbate species–adsorbent interactions, and adsorption is characterized by a uniform distribution of binding energies, up to some maximum binding energy [40].

$$q_e = \beta \ln K_t + \beta \ln C_e \quad (8)$$

where β is a constant representing the heat of adsorption $(= RT/b)$ and K_t is the equilibrium binding constant (L/g) corresponding to maximum binding energy. The linear plot of q_e *versus* $\ln C_e$ at three different temperatures (303, 313 and 323 K) for both the adsorption system gave good fit for the Temkin isotherm (Figure. 13). The values of K_t lie between 10.95-32.00 L/g (DR81-BSD) and 12.53-44.70 L/g (DR81-TBSD). The actual values of Temkin constants and R^2 are given in Table 3.

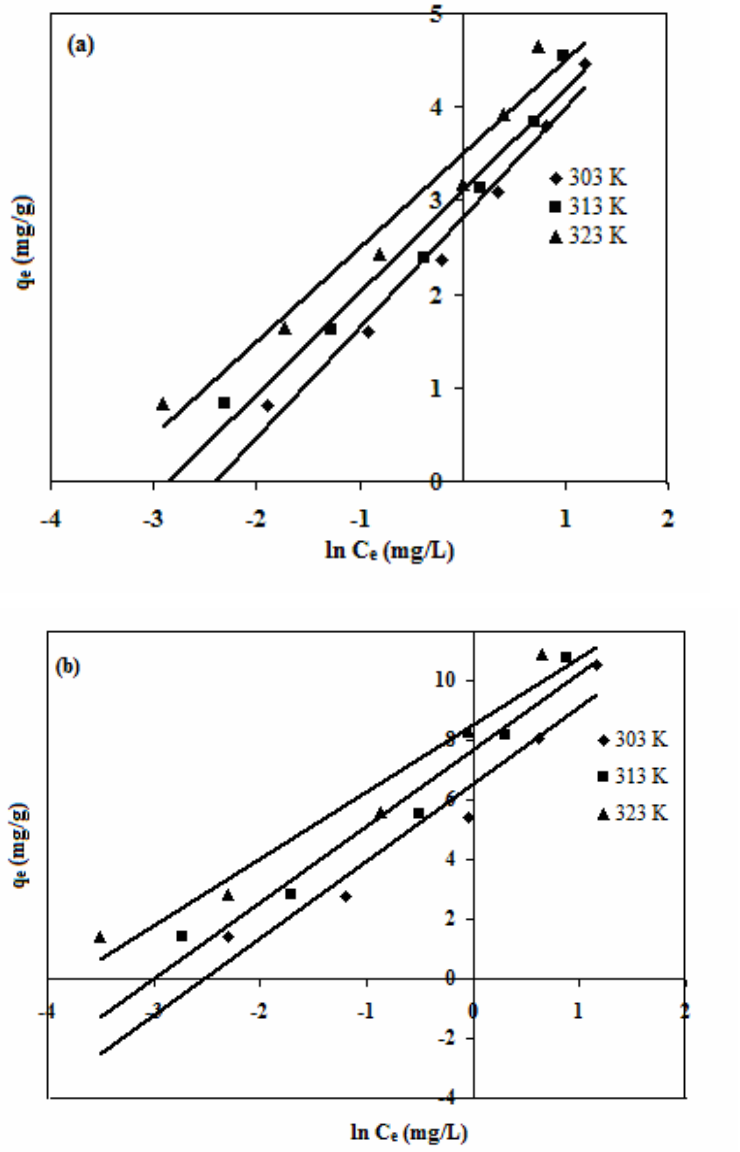

Figure 13. Temkin adsorption isotherm plots for adsorption of Direct Red 81 onto (a): bamboo sawdust and (b): treated bamboo sawdust.

3.8.5 Harkin-Jura isotherm

Harkin-Jura adsorption isotherm accounts for multilayer adsorption and can be explained by the existence of a heterogeneous pore distribution [41].

$$1/q_e^2 = (B/A)-(1/A) \log C_e \quad (9)$$

Where B and A are the isotherm constants. The Harkins-Jura isotherm parameters are obtained from the plots of $1/q_e^2$ *vs.* $\log C_e$ (Figure. 14). The values of Harkin-Jura constants and R^2 for both the adsorption system are given in Table 3.

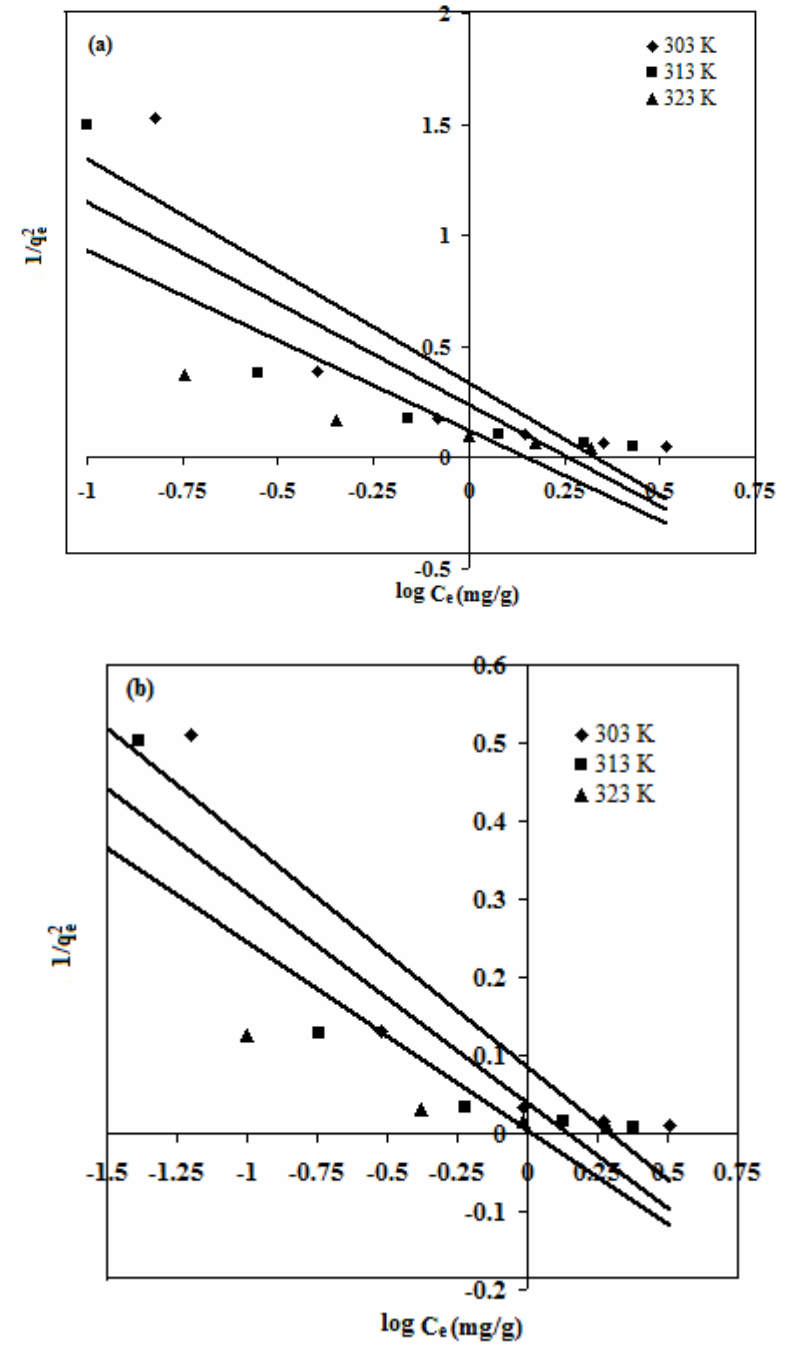

Figure 14. Harkin-Jura isotherm plots for adsorption of Direct Red 81 onto (a): bamboo sawdust and (b): treated bamboo sawdust.

3.8.6 Halsey isotherm

The Halsey adsorption isotherm can be given by Eq. (10) is suitable for multilayer adsorption [42, 43]. And the fitting of the experimental data to this equation show the hetero porous nature of the adsorbent.

$$\ln q_e = (1/n_h \ln K_h) - 1/n_h \ln C_e \quad (10)$$

Where K_h and n_h are the isotherm constants, and were obtained from the plot of $\ln q_e$ *vs.* $\ln C_e$ (Figure.15). The value of Halsey constants K_h and n_h along with R^2 of both the adsorption system are given in Table 3.

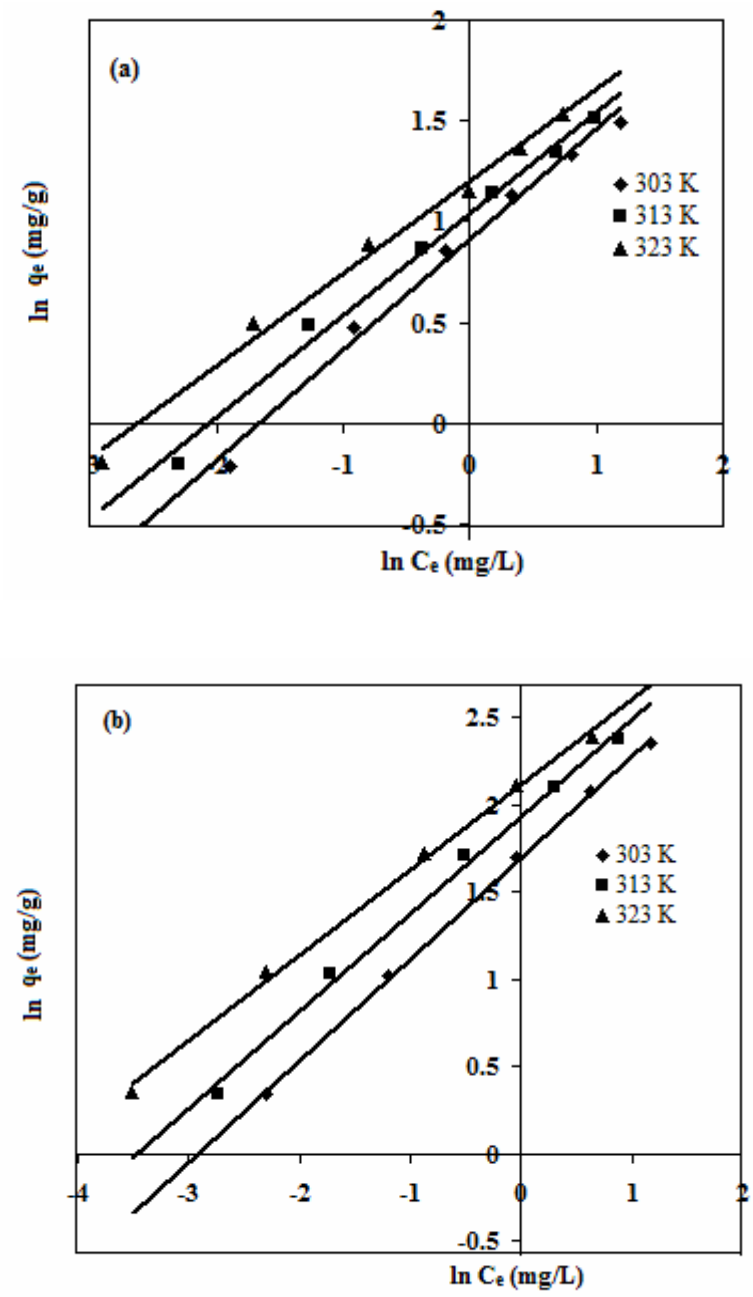

Figure 15. Halsey adsorption isotherm plots for adsorption of Direct Red 81 onto (a): bamboo sawdust and (b): treated bamboo sawdust.

The correlation factors and other parameters for Langmuir, Freundlich, Dubinin-Kaganer-Radushkevich, Temkin, Harkin-Jura and Halsey isotherm of both the adsorption system are presented in Table 3. The correlation factors confirm good agreement between theoretical models and our experimental results. The obtained data from both the adsorption system followed the six investigated isotherm models in the following order: Freundlich > Halsey > Langmuir > Temkin > Dubinin-Kaganer-Radushkevich > Harkin-Jura. The correlation coefficients for Freundlich and Halsey isotherms were highest in comparison to the values obtained from other isotherms and were a pointer to the heterogeneity of the surface of BSD and TBSD and the multilayer adsorption nature of the DR81 dye onto the adsorbents. Therefore, Freundlich and Halsey isotherm were found to best fit the equilibrium data for adsorption of dye on BSD and TBSD in both adsorption systems.

3.9 Thermodynamic Parameters

The energy and entropy considerations are very important in order to understand the kinetics of adsorption. The amount of dye adsorbed at equilibrium

and at different temperatures has been examined to obtain thermodynamic parameters for the adsorption system. The change in enthalpy (ΔH^o) and entropy (ΔS^o) are determined from the slope and intercept, respectively of the vant Hoff's plot $log\ (q_e/C_e)$ *vs* $1/T$ (Figure. 16), as given below:

$$log\ (q_e/C_e) = -\Delta H^o/2.303\ RT + \Delta S^o/2.303\ R \quad (11)$$

The free energy change (ΔG^o) was calculated from the following equation:

$$\Delta G^o = \Delta H^o - T\Delta S^o \quad (12)$$

Adsorption of dyes onto BSD and TBSD increases when temperature was increased from 303-323 K. ΔH^o, ΔS^o and ΔG^o for the adsorption process were computed from the plot between $log\ (qe/Ce)$ *vs.* $1/T$. Positive values of ΔH^o indicated endothermic nature of adsorption (Table 5). The positive mean values of ΔH^o for both the adsorption system 22.97 kJ/mol (DR81-BSD) and 35.02 kJ/mol (DR81-TBSD) at different dye concentrations indicated the endothermic nature of the interactions. And it was further suggested physisorption because the mean ΔH^o value obtained in this study was lower than 40 kJ/mol [44, 45]. The positive ΔS^o mean values of both the adsorption system 0.08 kJ/molK (DR81-BSD) and 0.13 kJ/molK (DR81-TBSD) favoured increased disorder and randomness at the solid-solution interface. The randomness might be attributed to the displaced water molecules gaining more translational entropy as compared to that lost by the dye molecules during the adsorption [46]. The Gibbs free energy was negative and increases towards negative side with rise in temperature, indicating the adsorption process to be spontaneous in nature and more favourable at higher temperature. Thus, the reaction was endothermic and spontaneous at all temperature.

Table 5.Thermodynamic parameters for adsorption of Direct Red 81 onto (a): bamboo sawdust and (b): treated bamboo sawdust.

Dye-Adsorbent	Conc. (mg/L)	ΔH^o (kJ/mol)	ΔS^o (kJ/mol K)	$-\Delta G^o$ (kJ/mol) 303 K	313 K	323 K
DR81-BSD	5	31.42	0.12	4.24	5.41	6.59
	10	30.64	0.11	3.45	4.58	5.71
	15	24.85	0.09	2.53	3.43	4.34
	20	14.13	0.05	1.98	2.51	3.04
	25	17.21	0.06	1.23	1.84	2.45
	30	19.59	0.06	0.72	1.39	2.06
DR81-TBSD	5	47.98	0.17	6.48	8.28	10.07
	10	44.23	0.16	5.54	7.18	8.83
	20	33.89	0.12	4.39	5.66	6.92
	30	27.40	0.10	3.66	4.69	5.71
	40	21.61	0.08	3.01	3.82	4.63

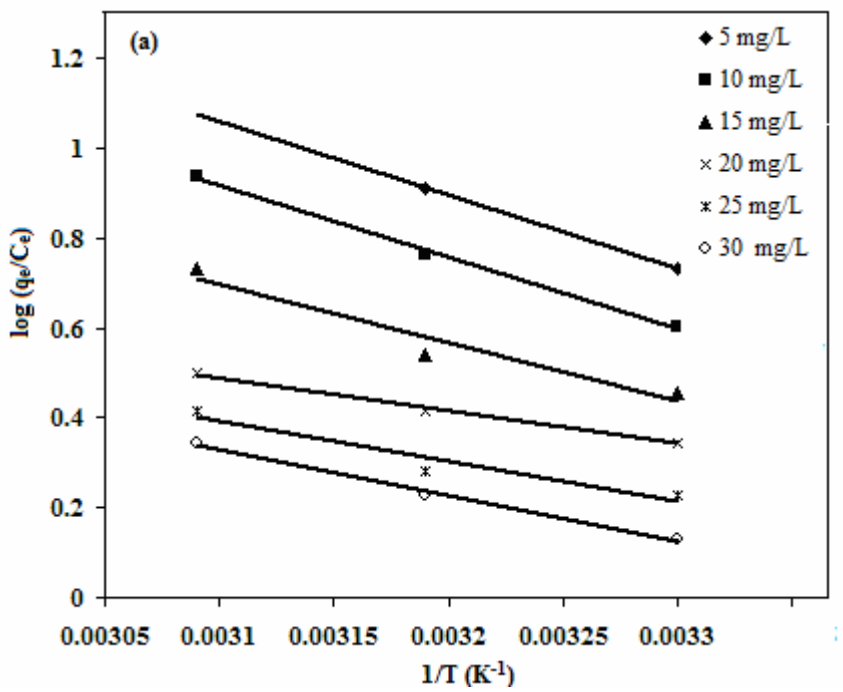

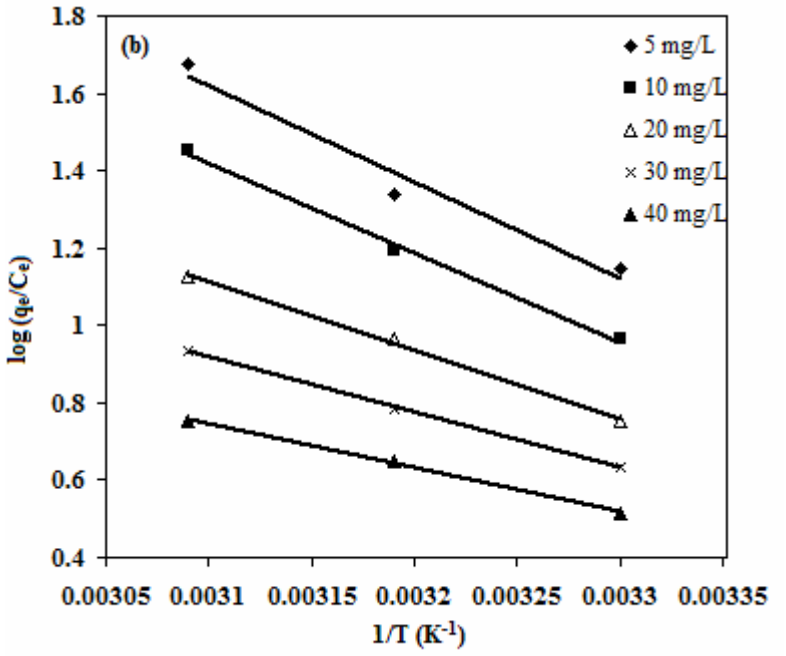

Figure 16. Plots of *log* (q_e/C_e) against *1/T* for adsorption of Direct Red 81 onto (a): bamboo sawdust and (b): treated bamboo sawdust.

3.10 Kinetic Studies

Five kinetics models have been used to investigate the mechanism of adsorption and potential rate controlling steps, which are helpful for selecting optimum operating conditions for the full-scale batch process.

3.10.1 Lagergren's pseudo-first order and pseudo-second order

The dynamics of the adsorption of DR81 dye onto BSD and TBSD were investigated using the Lagergren's pseudo-first order [47] (Eq. 13) and pseudo-second order equations [48] (Eq. 14).

$$log\ (q_e - q_t) = log\ q_e - k_1.t\ /(2.303) \quad (13)$$

$$t/q_t = 1/(\ k_2 q_e^2) + (1/q_e).t \quad (14)$$

where q_e and q_t are the amount of dye adsorbed per unit mass at equilibrium and at any time *t*, k_1 is the first-order adsorption rate constant (1/min), k_2 is the pseudo-second order rate constant (g/mg min) and h $(= k_2 q_e^2)$ is

the initial adsorption rate at time approaching 0 (mg/g min).

The k_1 and k_2 have been calculated from the intercept of the corresponding plots *of log* $(q_e - q_t)$ *vs. t* plot (Figure. 17), and *t/q vs. t* (Figure. 18), and are tabulated in Table 6 along with correlation coefficients and the q_e*(calc.)* and q_e*(exp.)* values. The correlation coefficient values for the pseudo-second order rate equation were higher than the pseudo-first order rate equation and also the theoretical q_e values were closer to the experimental q_e values. In the view of these results, it was confirmed that both the adsorption system followed pseudo-second order rate equation.

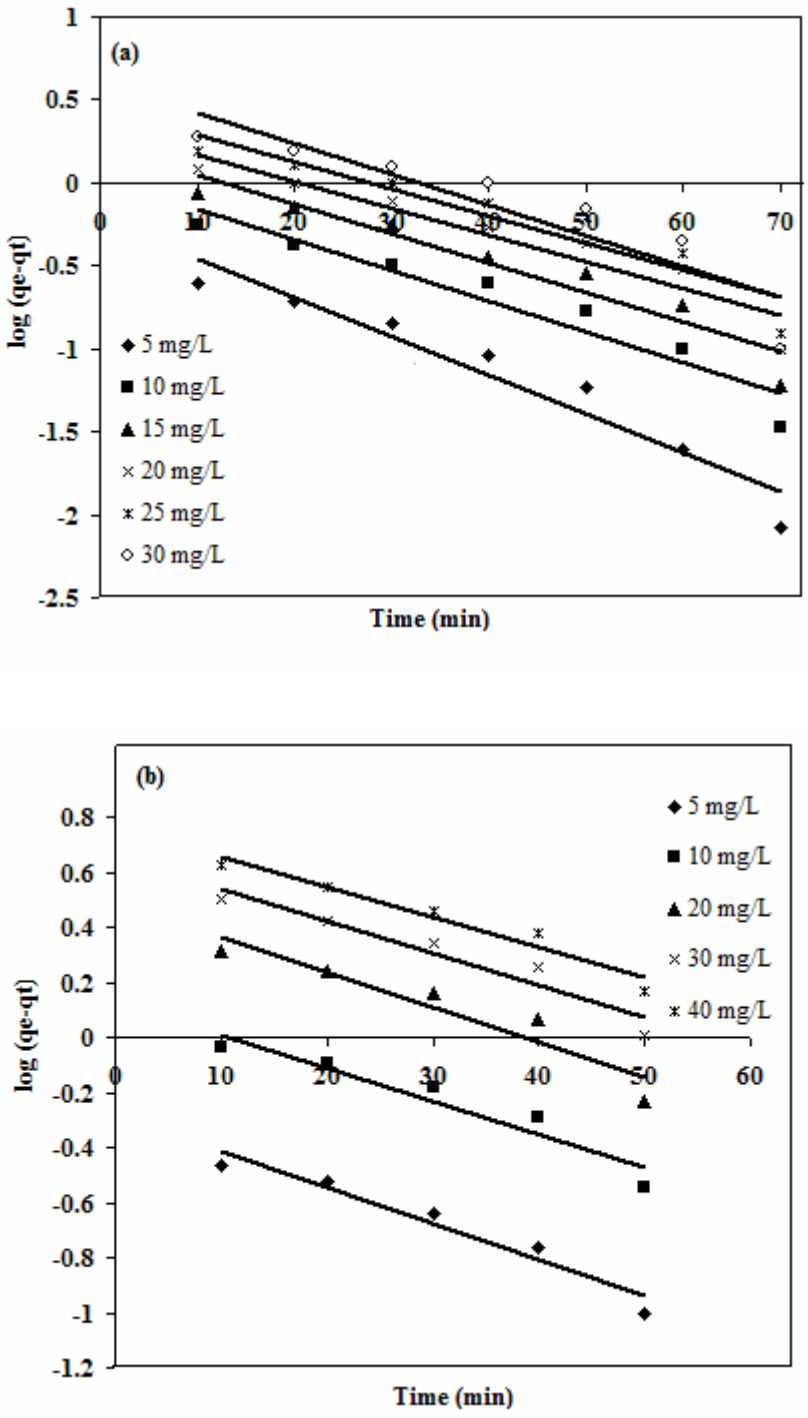

Figure 17. Pseudo-first order plots for adsorption of Direct Red 81 onto (a): bamboo sawdust and (b): treated bamboo sawdust.

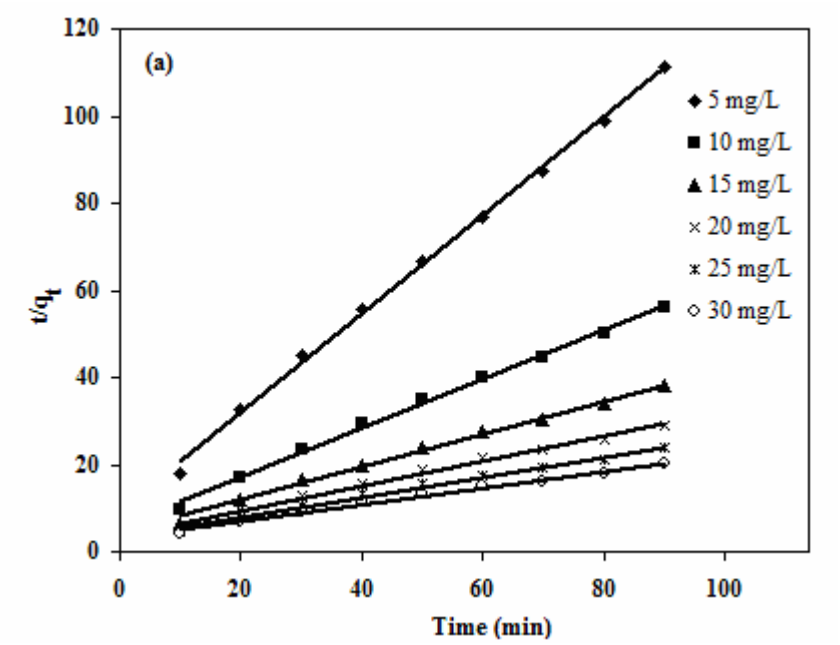

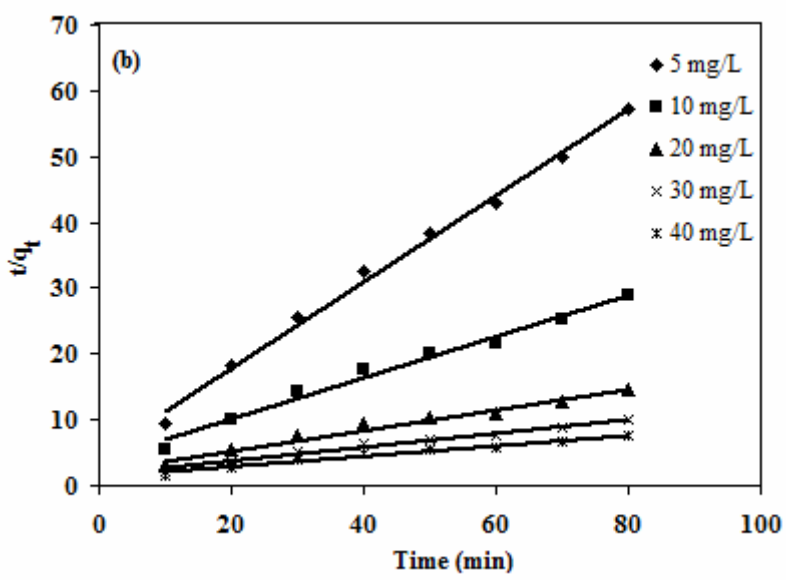

Figure 18. Pseudo-second order plots for adsorption of Direct Red 81 onto (a): bamboo sawdust and (b): treated bamboo sawdust

Table 6. Pseudo-first order and pseudo-second order rate constants values for the adsorption of Direct Red 81 onto (a): bamboo sawdust and (b): treated bamboo sawdust.

Dye-Adsorbent	Conc. (mg/L)	Pseudo-first order				Pseudo-second order		
		$k_1 \times 10^{-2}$ (1/min)	q_e (*calc)*(mg/g)	R^2	q_e (*exp)* (mg/g)	$k_2 \times 10^{-2}$ (g/mg min)	q_e (*calc)*(mg/g)	R^2
DR81-BSD	5	5.41	0.60	0.93	0.80	13.91	0.88	0.99
	10	4.26	1.05	0.91	1.60	5.65	1.76	0.99
	15	4.05	1.64	0.91	2.36	3.19	2.65	0.99
	20	3.73	2.15	0.90	3.10	2.17	3.51	0.99
	25	3.82	3.03	0.90	3.79	1.55	4.36	0.98
	30	4.23	4.01	0.83	4.45	1.18	5.20	0.98
DR81-	5	3.01	0.51	0.94	1.25	8.96	1.52	0.99
TBSD	10	2.76	1.35	0.91	2.37	2.65	3.17	0.98
	20	2.92	3.09	0.89	4.56	1.09	6.40	0.97
	30	2.67	4.48	0.92	6.69	0.68	9.54	0.97
	40	2.48	5.75	0.94	8.70	0.50	12.53	0.97

3.10.2 Elovich plot

The adsorption data may also be analyzed by using Elovich equation, which has the following form [49]:

$$q_t = 1/\beta.ln(\alpha.\beta) + 1/\beta\, ln(t) \quad (15)$$

where α (mg/g min) and β (g/mg) are the initial adsorption rate constant and desorption rate constant, respectively. Kinetics of adsorption of DR81 dye onto BSD and TBSD were also followed Elovich equation with the plots of q_t *vs. lnt* giving straight lines with high correlation coefficient (Figure. 19). The Elovich equation did not predict any definite mechanism, but it was useful in describing adsorption on highly heterogeneous adsorbents [49, 50]. The Elovich constants computed from the plots are given in Table 7. On comparing the correlation coefficients, it was found that the pseudo-second order kinetic model (R^2 = 0.97-0.99) describe the adsorption data better than Elovich model for both the adsorption system.

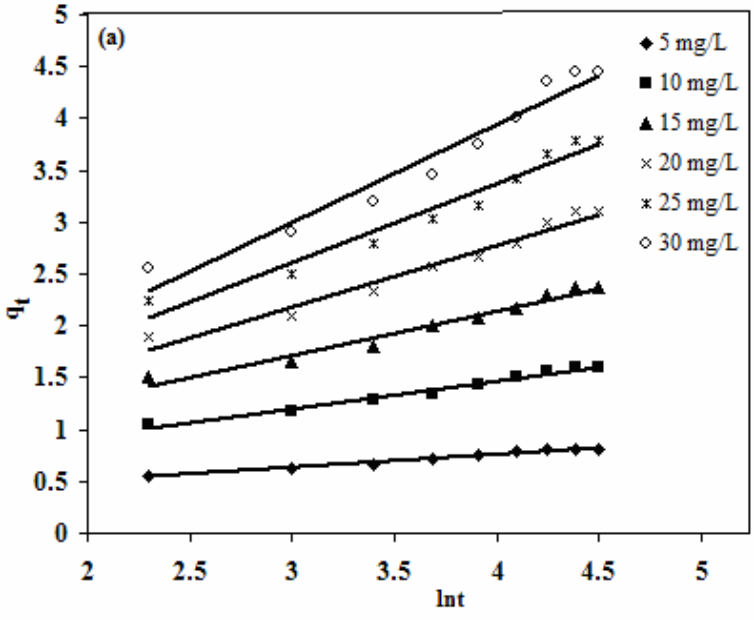

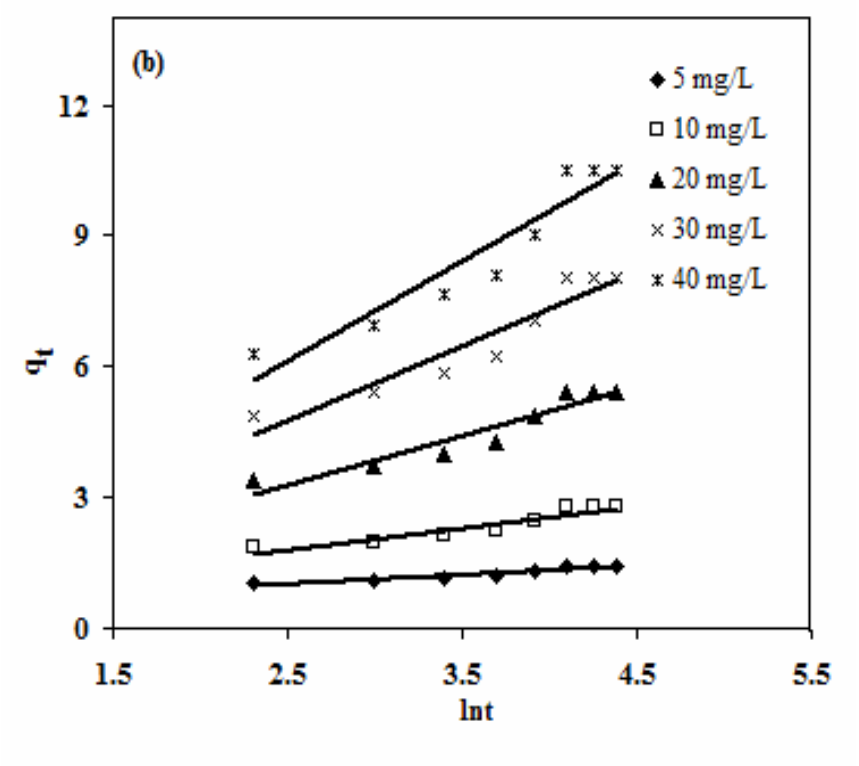

Figure 19. Elovich plots for adsorption of Direct Red 81 onto (a): bamboo sawdust and (b): treated bamboo sawdust.

Table 7. Elovich, liquid-film diffusion and intra-particle diffusion rate constants values for the adsorption of Direct Red 81 onto (a): bamboo sawdust and (b): treated bamboo sawdust.

Dye-Adsorbent	Conc. (mg/L)	Elovich			Liquid-film diffusion		Intra-particle diffusion		
		α (mg/gmin)	β (g/mg)	R^2	$K_{fd} \times 10^{-2}$ (1/min)	R^2	K_i (mg min$^{0.5}$/g)	C_i	R^2
DR81-BSD	5	0.95	7.95	0.98	5.42	0.93	0.04	0.43	0.97
	10	1.16	3.72	0.98	4.25	0.94	0.09	0.77	0.98
	15	1.13	2.31	0.96	4.05	0.91	0.14	1.02	0.98
	20	1.17	1.68	0.96	3.73	0.90	0.20	0.23	0.99
	25	1.14	1.30	0.95	3.76	0.88	0.26	1.36	0.98
	30	1.10	1.05	0.95	4.25	0.83	0.32	1.45	0.98
DR81-	5	3.79	5.28	0.91	3.77	0.85	0.06	0.81	0.95
TBSD	10	1.46	1.97	0.89	3.42	0.80	0.18	1.18	0.94
	20	1.69	0.88	0.90	3.61	0.78	0.41	1.91	0.94
	30	2.23	0.58	0.89	3.31	0.82	0.62	2.65	0.94
	40	2.72	0.43	0.89	3.12	0.86	0.83	3.33	0.94

3.10.3 Liquid-film diffusion

Liquid-film diffusion can be explained by the following equation [51]:

$$-ln(1-F) = K_{fd}\,t \qquad (16)$$

where F is the fractional attainment of equilibrium ($F = q_t/q_e$) at time t, and K_{fd} (1/min) is the adsorption rate constant. The plots of $ln(1-F)$ *vs.* t (Figure. 20) for both the adsorption system were also linear. The rate constant for liquid-film diffusion, K_{fd}, were in the range of 3.73-5.42 × 10^{-2} 1/min (DR81-BSD) and 3.12-3.77 × 10^{-2} 1/min (DR81-TBSD) of both the adsorption system (Table 7). The plots, however, did not pass through the origin. Thus, the liquid-film diffusion was not the only predominant mechanism for DR81 dye adsorption onto BSD and TBSD.

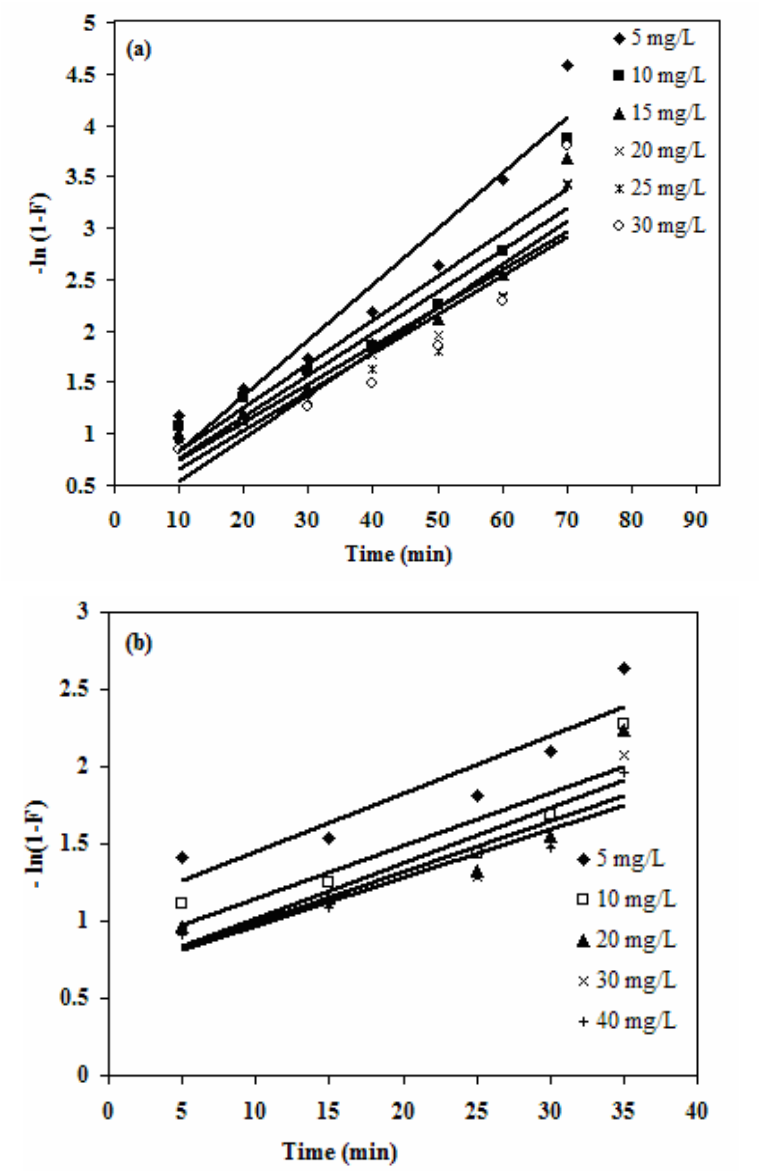

Figure 20. Liquid-film diffusion plots for adsorption of Direct Red 81 onto (a): bamboo sawdust and (b): treated bamboo sawdust.

3.10.4 Intra-particle diffusion

The variation in the amount of adsorption with time at different initial dyes concentrations could be further processed for evaluating the role of diffusion in the adsorption process. Adsorption is a multi-step process involving transport of the solute molecules from the aqueous phase to the surface of the solid particulates followed by diffusion of the solute molecules into the pore interiors. The intra-particle diffusion rate is given by the equation [52]:

$$q_t = k_i t^{0.5} + C_i \quad (17)$$

where k_i (mg/g $min^{0.5}$) and C_i are the intra-particle diffusion rate constant and boundary layer thickness, respectively. The effect of pore diffusion on the adsorption process was tested by plotting q_t *vs.* $t^{0.5}$ (Figure. 21). All the plots of both the adsorption system have the same general features of an initial curved portion followed by a linear portion and a plateau. The initial curved portions were attributed to the bulk diffusion, the linear portion to the intra-particle diffusion and the plateau to the equilibrium. The magnitudes of k_i, C_i and the corresponding regression coefficients of both the adsorption system are listed in Table 7. The pore diffusion rate constant, k_i, values indicated substantial diffusion of DR81 dye onto BSD and TBSD adsorbent. However, the plots did not pass through the origin, so it might not be the only controlling factor in determining the kinetics of the process. It may be inferred that both the liquid-film and intra-particle diffusion might be controlling the kinetics of the DR81-BSD and DR81-TBSD interactions.

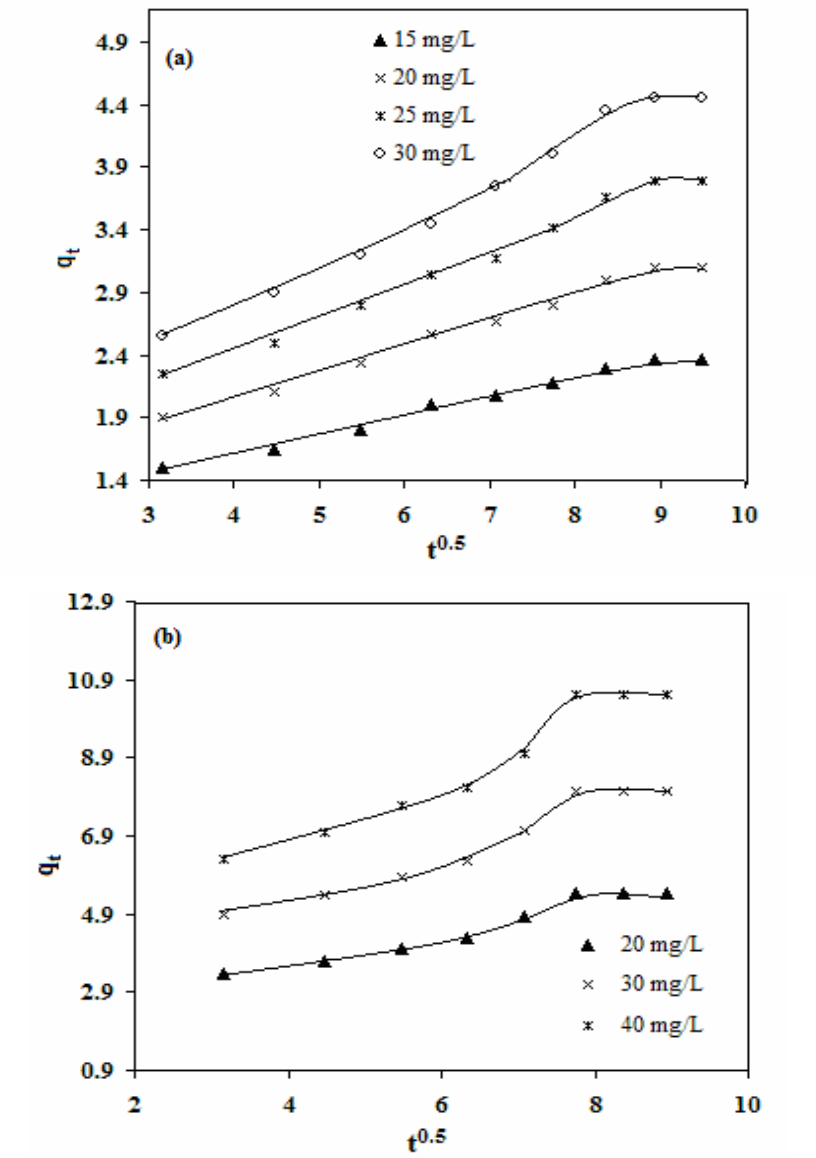

Figure 21. Plots of q_t *vs.* $t^{0.5}$ for adsorption of Direct Red 81 onto (a): bamboo sawdust and (b): treated bamboo sawdust.

The kinetics of interactions tested with Lagergren pseudo-first and pseudo-second order kinetics, Elovich equation, liquid-film and intra-particle diffusion mechanism of the both adsorption system. It was observed that pseudo-second order kinetic model described the adsorption process with higher coefficients of determination better than any other kinetic models of both the adsorption system. The mechanism of removal of DR81 dye by BSD and TBSD was controlled by both liquid-film and intra-particle diffusion.

4. CONCLUSION

This study confirmed that BSD and TBSD, a low-cost cellulose-based waste, could effectively remove Direct Red 81 dye from aqueous solution. Maximum adsorption capacity (q_m) obtained from the Langmuir isotherm plots were 6.43 mg/g (89%) (DR81-BSD) and 13.83 mg/g (92%) (DR81-TBSD) at 303 K. The monolayer adsorption capacity for the citric acid treated bamboo sawdust was higher as compared to that obtained without chemical treatment. The adsorbents, before and after adsorption, were characterized by fourier transform infrared spectrometer, X-ray diffraction and scanning electron microscope. FTIR investigation of BSD and TBSD before and after adsorption showed many changes and shifts in peaks, indicating the dye binding process taking place on the surface of the adsorbent. The obtained data followed the six investigated isothermal models in the following order: Freundlich > Halsey > Langmuir > Temkin > Dubinin-Kaganer-Radushkevich > Harkin-Jura. The pseudo-second order kinetic model described the data best than pseudo-first order, due to the high correlation coefficient values and the agreement between the experimental and calculated values of q_e. Thermodynamic parameters (ΔG^o, ΔH^o and ΔS^o) suggested the adsorption process to be spontaneous and endothermic. It was observed that both liquid-film and intra-particle diffusion controlled the overall kinetics of the adsorption process in both the adsorption system. The developed adsorption system is inexpensive, eco-friendly and efficient for the removal of dye from any water due to its small adsorption time, good capacity of adsorption of adsorbent and working at 7 pH; a natural pH of most of natural water resources.

5. ACKNOWLEDGEMENT

One of the authors (S. Dahiya) is thankful to University Grants Commission (UGC) New Delhi 110 025, India for awarding fellowship.

REFERENCES

[1] Gupta, V.K., Carrott, P.J.M. and Ribeiro Carrott, M.M.L., "Low-Cost adsorbents: Growing approach to wastewater treatmenta review", ***Crit. Rev. Environ. Sci. Technol***., 39: 783-842 (2009).

[2] Gupta, V.K. and Suhas' "Application of low-cost adsorbents for dye removal - A review", ***J. Environ. Manage.***, 90: 2313-2342 (2009).

[3] Mathur, Nupur, Pradeep and Bhatnagar, P., "Mutagenicity assessment of textile dyes from Sanganer (Rajasthan)", ***J. Environ. Biol.,*** 28: 123-126 (2007).

[4] Stephenson, R.J. and Sheldon, J.B., "Coagulation and precipitation of mechanical pueffluent. 1. Removal of carbon and turbidity", ***Water Res.,*** 30: 781-792, (1996).

[5]. Ali I., "The quest for active carbon adsorbent substitutes: Inexpensive adsorbents for toxic metal ions removal from wastewater", ***Sepn. & Purfn***. ***Rev***., 39: 95-171, (2010).

[6]. Ali, I., and Gupta, V.K., "Advances in Water Treatment by Adsorption Technology", ***Nature London,*** 1: 2661-2667, (2006).

[7]. Gupta, V.K., Mittal, A., Gajbe, V. and Mittal, J., **"**Removal and recovery of the hazardous azo dye acid orange 7 through adsorption over waste materials: Bottom ash and de-oiled soya", ***Ind. & Eng. Chem. Res.***, 45: 1446-1453, (2007).

[8] Gupta, V.K., Mittal, A., Krishnan, L. and Mittal, J., **"**Adsorption treatment and recovery of the hazardous dye, Brilliant Blue FCF, over bottom ash and de-oiled soya", ***J. Colloid Interface Sci.,*** 293: 16-26, (2006).

[9] Gupta, V.K., Mittal, A., Gajbe, V. and Mittal, J., **"**Adsorption of basic fuchsin using waste materials-bottom ash and deoiled soya-as adsorbents", ***J. Colloid Interface Sci.***, 319: 30-39, (2008).

[10] Gupta, V.K., Ali, i., Saini, V.K., Gerven, T.V., Van der Bruggen, B. And Vandecasteele, C., "Removal of dyes from wastewater using bottom ash", ***J. Ind. & Eng. Chem. Res.,*** 44: 3655-3664, (2005).

[11] Mittal, A., Kurup, L. and Gupta, V.K., "Use of waste materials - Bottom ash and de-oiled soya, as potential adsorbents for the removal of amaranth from aqueous solutions", ***J. Hazard. Mater.***, 117: 171-178, (2005).

[12]. Khan, T.A., Ali, I., Singh, V. and Sharma, S., "Utilization of fly ash as low-cost adsorbent for the removal of methylene blue, malachite green and rhodamine B dyes from textile wastewater", ***J. Environ. Prot. Sci.,*** 3: 11-22, (2009).

[13]. Khan, T.A., Singh, V. and Kumar, D., "Removal of some basic dyes from artificial textile wastewater by adsorption onto akash kinari coal", ***J. Sci. Ind. Res.,*** 63: 355-364, (2004).

[14]. Gupta, V., Mohan, D. and Sharma, S., "Removal of lead from wastewater using bagasse fly ash - a sugar industry waste material", ***Sep. Sci. Technol.***, 33: 1331-1343, (1998).

[15]. Gupta, V.K., Ali, I. and Saini, V.K., "Adsorption studies on the removal of vertigo blue 49 and orange DNA13 from aqueous solutions using carbon slurry developed from a waste material", ***J. Colloid Interface Sci.,*** 315: 87-93, (2007).

[16]. Gupta, V.K., Jain, R. and Varshney, S., "Removal of reactofix golden yellow 3 RFN from aqueous solution using wheat husk-An agricultural waste", ***J. Hazard. Mater.,*** 142: 443-448, (2007).

[17] Gupta, V.K. and Rastogi**,** A., "Equilibrium and kinetic modelling of cadmium(II) biosorption by nonliving algal biomass Oedogonium sp. from aqueous phase", ***J. Hazard. Mater.,*** 153: 759-766, (2008).

[18] Venkata Mohan, S., Chandrasekhar Rao, N. and Karthikeyan, J., "Adsorptive removal of direct azo dye from aqueous phase onto coal based sorbents: a kinetic and mechanistic study", ***J. Hazard. Mater.,*** 90: 189-204, (2002).

[19] Namasivayam, C., Prabha, M. and Kumutha, D., "Removal of congo red from water by adsorption onto activated carbon prepared from coir pith, an agricultural solid waste", ***Bioresour. Technol***., 64: 77-79, (1988).

[20]. ABSDelwahab, El Nemr A., El Sikaily A. and Khaledegyptian, A., "Use of Rice Husk for adsorption of direct dyes from aqueous solution: A Case Study Of Direct F. Scarlet", ***J. Aquatic Res.,*** 31: 1-11, (2005).

[21]. Namasivayam, C. and Kavitha, D., "Removal of congo red from water by adsorption onto activated carbon prepared from coir pith, an agricultural solid waste", ***Dyes Pigs.,*** 54: 47-58, (2002).

[22] Gupta, V.K., Mittal, A., Jain, R., Mathur, M. and Sikarwar, S., "Adsorption of Safranin-T from wastewater using waste materials- activated carbon and activated rice husks", ***J. Colloid Interface Sci.***, 303: 80-86, (2006).

[23] Stuart, B., "Modern Infrared Spectroscopy", ***Wiley***, Chister, UK, (1996).

[24]. Malik, P.K., "Dye removal from wastewater using activated carbon developed from sawdust: Adsorption equilibrium and kinetics", ***J. Hazard. Mater.,*** 113: 81-88, (2004).

[25]. Mohamed, M.M., "Acid dye removal: Comparison of surfactant-modified mesoporous FSM-16 with activated carbon derived from rice husk", ***J. Colloid Interface Sci.***, 272: 28-34, (2004).

[26] Khattri, S.D. and Singh, M.K., "Removal of malachite green from dye wastewater using neem sawdust by adsorption", ***J. Hazard. Mater.,*** 167: 1089-1094, (2009).

[27] Baztias, F.A. and Sidiras, D.K., "Dye adsorption by prehydrolysed beech sawdust in batch and fixed-bed systems", ***Biores. Technol.***, 98: 1208-1217, (2007).

[28] Chiou, M.S., Ho, P.Y. and Li, H.Y., "Adsorption of anionic dyes in acid solutions using chemically cross-linked chitosan beads", ***Dyes Pigs.,*** 60: 69-84, (2004).

[29] Ozacar, M. and Sengil, I.A., "Adsorption of reactive dyes on calcined alunite from aqueous solutions", J. Hazard. Mater., 98: 211-224 (2003).

[30]. Gupta, V.K., Ali I., Suhas and Mohan D., "Equilibrium uptake sorption for the removal of a basic dye (basic red) using low cost adsorbent", ***J. Colloid Interface Sci***., 265: 257-264, (2003).

[31] Srivastava, R. and Rupainwar, D.C., "Eucalyptus bark powder as an effective adsorbent: Evaluation of adsorptive characteristics for various dyes", ***Desalination Water Treatment***, 11: 302-313, (2009).

[32] Langmuir, I., "The adsorption of gases on plane surfaces of glass, mica, and platinum", ***J. A. M. Chem***. ***Soc.***, 40: 1361-1403, (1918).

[33] Hall, K.R., Eagleton, L.C., Acrivos, A. and Vermeulen, T., "Pore and solid-diffusion kinetics in fixed-bed adsorption under constant-pattern conditions", ***Ind. Eng. Chem. Fund.***, 5: 212-223, (1966).

[34]. Yavuz, Ö. and Aydin, A.H., "Removal of direct dyes from aqueous solution using various adsorbents", ***Polish J. Environ. Studies***, 15: 155-161, (2006).

[35]. Venkata Mohan, S., Chandrasekhar Rao, N. and Karthikeyan, J., "Adsorptive removal of direct azo dye from aqueous phase onto coal based sorbents: a kinetic and mechanistic study", ***J. Hazard. Mater.,*** 90: 189-204, (2002).

[36] Martin, M.J., Artola, A., Balaguer, M.D. and Rigola, M., "Activated carbons developed from surplus sewage sludge for the removal of dyes from dilute aqueous solution", ***Chem. Eng. J.,*** 94: 231-239, (2003).

[37] Namasivayam, C. and Arasi, D.J.S.E., "Removal of congo red from wastewater by adsorption onto red mud", ***Chemosphere,*** 34: 401-471, (1997).

[38]. Freundlich, H.Z., "Over the adsorption in solution", ***J. Phys. Chem.,*** 57: 385-470, (1906).

[39] Dubinin, M.M. and Radushkevich, L.V., "The equation of the characteristic curve of activated charcoal", ***Dokl. Akad. Nauk Sssr***, 55: 327-329 (1947).

[40]. Temkin, M.I. and Pyzhev, V., "Kinetic of ammonia synthesis on promoted iron catalyst", ***Acta physiochim.*** USSR, 12: 327-356, (1940).

[41]. Harkins, W.D. and Jura, G.J., "The decrease of free surface energy as a basis for the development of equations for adsorption isotherms; and the existence of two condensed phases in films on solid", ***J. Chem. Phys***., 12: 112-113, (1944).

[42]. Halsey, ***J. Chem. Phys.***, 16: 931, (1948).

[43] Basar, C.A., "Applicability of the various adsorption models of three dyes adsorption onto activated carbon prepared from waste apricot", ***J. of Hazard Mater.,*** 135: 232-241 (2006).

[44]. Ponnusami, V., Aravindhan, R., Karthik raj, N., Ramadoss, G. and Srivastava, S. N., "Adsorption of methylene blue onto gulmohar plant leaf powder: Equilibrium, kinetic, and thermodynamic analysis", ***J. Environ. Prot. Sci***., 3: 1-10, (2009).

[45] Bhatnagar, A., Kumar, E., Minocha, A. K., Jeon, B.H., Song, H. and Seo, Y.C., Removal of anionic dyes from water using citrus limonum (lemon) peel: Equilibrium studies and kinetic modelling", ***Sep. Sci. Technol.,*** 44: 316-334, (2009).

[46]. Gopal, V. and Elango. P., "Kinetic and thermodynamic investigations of adsorption of fluoride onto activated aloe vera carbon", ***J. Indian Chem. Soc.,*** 84: 1114-1118, (2007).

[47] Lagergren, S., "About the theory of so-called adsorption of soluble substances", ***K. Sven.Vetenskapsakademiens. Handl.,*** 24: 1-39, (1898).

[48] Ho, Y.S. and McKay, G., "Pseudo-second order model for sorption processes", ***Process Biochem***., 34: 451-465 (1999).

[49]. Chien, S.H. and Clayton, W.R., "Application of elovich equation to the kinetics of phosphate release and sorption on soils", ***Soil Sci. Soc. Am. J.*** 44: 265-268, (1980).

[50]. Ho, Y.S. and Mckay, G., "Comparative sorption kinetic studies of dyes and aromatic compounds onto fly ash", ***J. Environ. Sci. Heal.,*** 34: 1179-1204, (1999).

[51]. Boyd, G.E., Adamson, A.M. and Myers, L.S., "The exchange adsorption of ions from aqueous solution bioorganic zeolites II, Kinetics", ***J. Am. Chem. Soc.***, 69: 2836-2842, (1949).

[52]. Weber, W.J. and Morris, J.C., "In: Eckenfelder W.W. (Ed.), Advances in water pollution research", ***Pergamon Press,*** Oxford, (1964).